



Supplement of

Modeling regional aerosol and aerosol precursor variability over California and its sensitivity to emissions and long-range transport during the 2010 CalNex and CARES campaigns

J. D. Fast et al.

Correspondence to: J. D. Fast (jerome.fast@pnnl.gov)

This supplement contains additional tables and figures that summarize model performance at surface sampling sites and along aircraft flight paths and ship tracks. Statistical metrics in the tables include the bias, root-mean-square error (RMSE), correlation coefficient (R), and index of agreement (IA) for various meteorological, trace gas, and aerosol quantities.

Aerosol Modeling Testbed

The extensive data collected during CalNex and CARES are an ideal testbed for evaluating photochemical and aerosol models; therefore, they have been merged into a single dataset used by the Aerosol Modeling Testbed (AMT). The AMT [*Fast et al.*, 2011] consists of a host model, testbed cases, and post-processing software. The host model is the Weather Research and Forecasting (WRF-Chem) community model [*Skamarock et al.*, 2005] that permits on-line coupling of meteorology and chemistry [*Grell et al.*, 2005; *Fast et al.*, 2006]. Since detailed measurements of aerosol properties are not routinely collected aloft, the AMT uses meteorological, trace gas, and aerosol measurements from field campaigns to define each testbed case. The analysis software extracts simulated variables in a manner compatible with the available measurements using “instrument simulators”. Examples of instrument simulators include the interpolation of model output in space and in time along research aircraft flight tracks and over vertical profiles sampled by radar wind profilers and lidars. Statistical and graphical programs are also available in the analysis software. While the AMT has been designed for use with WRF, the analysis software can be modified for other models. For example, *Ensberg et al.* [2013] used the AMT software coupled with the Community Multiscale Air Quality (CMAQ) modeling system to evaluate simulated aerosol concentration and composition in the Los Angeles Basin using the CalNex CIRPAS Twin Otter measurements.

The field campaign and operational data used for the CalNex/CARES testbed case have been provided through several archives with a variety of formats (e.g. ASCII, ICARTT, NetCDF, HDF, Microsoft Excel). Modelers need to write software that handles the variety of formats, which usually changes from field campaign to field campaign. Inevitably, each user that processes the same field dataset creates different software scripts or programs. As part of the AMT, a common ASCII format is employed for most of the data and data has been organized into common types including surface, aircraft, profile, and satellite. Subdirectories are created for each supersite or operational network in the case of surface instrumentation, and for each research aircraft in the case of airborne sampling. The directory structure for the AMT CalNex/CARES

testbed case is given in Fig. S1. Some of the sub-directories contain data exclusively from CalNex or CARES, while other sub-directories contain data from both campaigns, e.g., in the case of instrument platforms participating in both, such as the B-200 and NOAA Twin Otter aircraft. In addition to data from the radiosonde, radar wind profiler, CARB, IMPROVE, AERONET networks, satellite measurements of aerosol optical depth from the Moderate Resolution Imaging Spectroradiometer (MODIS) on the Aqua and Terra satellites are also included in the testbed case. An identical directory structure is employed for model output extracted to be temporally and spatially compatible with the measurements, enabling graphics and statistics to evaluate model performance. In this way, the AMT permits users to spend more time on science issues (rather than on tedious and repetitive tasks associated with data processing), target specific aerosol processes and other atmospheric processes affecting aerosol evolution, and document improvements in parameterizations.

The testbed case containing the CARES and operational data as well as the analysis toolkit software is available to download from the Atmospheric Radiation Measurement (ARM) research climate facility archive at <http://www.arm.gov/data/eval/59>. Users are encouraged to contact Jerome Fast (Jerome.Fast@pnnl.gov) for an updated version of the dataset.

Evaluation of Meteorological Quantities

Since the current model configuration is somewhat different than previous studies [*Angevine et al., 2012; Fast et al., 2012*], some comparisons of observed and simulated temperature, humidity, wind speed and direction, and solar radiation from the DEF_ANT simulation are presented here to demonstrate the performance of the model in representing the meteorological conditions that affect the vertical mixing, transport, chemical transformation, and removal of trace gases and aerosols.

An example of the simulated surface meteorology at the Pasadena supersite over May and June of 2010 as well as the diurnal averages is shown in Fig. S2. The model is able to reproduce the multi-day variability of temperature and relative humidity although the simulated nighttime temperatures are a few degrees warmer than observed and the relative humidity is generally 10% lower than observed at all times of the day. As seen in the solar radiation, the mostly sunny conditions occurred on the majority of the days. While the model correctly produces clouds on some days when they occurred (May 17 – 18, June 8-9, the overall reduction in downward shortwave radiation due to clouds is less than observed suggesting that the simulated liquid or ice water path is too low. The near-surface winds at Pasadena exhibit nearly the same diurnal variation from day to day, with southwesterly winds during the day that become

weaker and southerly to southeasterly at night. While the model reproduces the diurnal variability in wind direction, the predicted wind speeds are too high. The over-prediction in wind speeds is likely due to two factors: 1) urban canopy effects that are not included in the current model configuration of the model, and 2) sub-grid scale terrain effects since the site is located near the edge of the San Gabriel Mountains. The performance of near surface winds is usually better at other stations located outside of urban areas and/or in flat terrain (not shown).

Table 4 summarizes statistics that quantify model performance for the simulated near-surface temperature, relative humidity, wind speed, and wind direction average over California and averaged over smaller geographic regions depicted in Fig. 1c. As with the Pasadena site, simulated temperatures are usually 0.2 to 0.9 K too low and the diurnal and multi-day temporal variations are similar to observations. Relatively humidity is usually lower than observed by 5.5 to 7.0% over the San Joaquin Valley and southern California, but is generally within 1% of the observations on average elsewhere. Simulated near surface wind speeds are usually higher than observed with the largest biases for stations in the “coastal” region. The average bias in wind direction is less than 10 degrees for the San Joaquin Valley, Sacramento Valley, and coastal regions, but between 17.6 and 22.5 degrees over southern California and the interior mountains. While the model qualitatively captures the diurnal and multi-day variability in wind direction, it is not surprising that it cannot represent the high frequency variations especially when wind speed are low ($< 1 \text{ m s}^{-1}$) as shown in Fig. S2e. This is the primary reason for the low wind direction correlations in Table 4.

Statistics summarizing the performance in simulated temperature, relative humidity, wind speed, and wind direction for all of the G-1, CIRPAS Twin Otter, and WP-3D flight paths and the R/V Atlantis deployment are shown in Table 5. In general, the spatial and temporal variability in temperature in the lower troposphere is reasonably simulated as reflected by the relatively high correlation coefficients that are similar to the surface measurements; however, the model is 2 to 3 degrees colder than observed on average. Conversely, the near surface temperatures over the ocean are about 1 degree warmer on average than those from the R/V Atlantis. The relative humidity statistics are similar to those at the surface measurement sites with the model being 4 to 7% drier than observed, except along the G-1 flight paths that had a very small bias. The wind speeds aloft along the G-1 and WP-3D flight paths are very similar to observed and consequently the errors are much smaller than at the surface measurement sites. Nevertheless, the correlation coefficients indicate that the model did not represent all of the spatial and temporal variability in wind speed. Wind speed variability is better represented over southern California where the WP-

3D usually flew than over northern California where the G-1 flew. Statistics for individual aircraft flights and daily statistics for the R/V Atlantis sampling are given in Tables S1 – S14.

It is also important to evaluate the evolving simulated winds throughout the boundary layer and lower troposphere when assessing the ability of a model to simulate horizontal transport downwind of emissions sources; therefore the simulated winds aloft have been evaluated with measurements from the radar wind profiler network shown in Fig. 1c. While *Fast et al.* [2012] demonstrated that the observed and simulated wind speed and direction, associated with varying synoptic conditions and thermally-driven flows, was similar in the vicinity of Sacramento during June, this study quantifies model performance over all of California for May and June. Statistics that summarize the model performance at all the radar wind profiler sites at three altitudes are given in Tables 6 and 7. The performance varies among the sites and with altitude as expected. Figure S3 shows the observed and simulated diurnally-averaged winds over May and June of 2010 at the Sacramento, Bakersfield, and USC radar wind profilers based on the time series shown in Fig. S4. The simulated wind speed and direction at Sacramento (Fig. S2a) is very close to observed, except for a few periods during the night that differ by as much as 30 degrees. Both the observed and simulated winds at Bakersfield are usually northwesterly all day (Fig S2b), but the model overestimates the wind speeds at night. Low-level jets frequently occur in the San Joaquin Valley, but the simulated wind speeds are too strong on some nights consistent with *Bao et al.* [2008] in their WRF simulation of winds during the Central California Ozone Study. At USC (Fig. S2c), the model reproduces the overall diurnal variation in wind speed and direction at this altitude, but the wind speeds are generally $1\text{-}2 \text{ m s}^{-1}$ higher than observed during the night and early morning and the simulated wind directions are more westerly than observed. When comparing Fig. S2d and Fig. S4c, the daytime wind speed bias decreases significantly with height, but the bias at night is similar at both altitudes.

Boundary-layer depth is an important meteorological quantity, since it defines the vertical extent of turbulent mixing that dilutes the concentrations of near-surface trace gases and aerosols and alters chemical transformation. The performance of the model in simulated boundary-layer depth compared with the radiosondes collected at the T0 and T1 sites is nearly identical to *Fast et al.* [2012] and is not included here. *Scarino et al.* [2013] present a methodology of deriving boundary layer heights from backscatter profiles measured by the HRSL on the B-200 aircraft. An advantage of this data set is that the simulated spatial and temporal variability in boundary layer height can be evaluated, as opposed to comparing model predictions to infrequent soundings made at a few locations. *Scarino et al.* [2013] use the results from the DEF_ANT simulation to show that the simulated spatial and temporal variations in boundary layer depths are usually

similar to those derived along the B-200 aircraft flight paths. Statistics that summarize the model performance during the day also show that the model boundary layer depths are somewhat too low over southern California during the CalNex flights, but are closer to observed over northern California during the CARES flights.

Table S1. Performance of simulated temperature (T) in terms of bias, RMSE, R, and IA for the individual G-1 aircraft flight paths.

Variable	Flight Date	Number of Data Points	Observed				
			Mean	Bias	RMSE	R	IA
T (K)	June 03a	849	292.0	-2.9	3.1	0.96	0.69
	June 06a	1164	296.3	-4.0	4.3	0.39	0.33
	June 06b	989	296.1	-4.5	4.7	0.97	0.85
	June 08a	1170	293.2	-2.4	3.3	0.27	0.47
	June 08b	1213	292.7	-5.0	5.5	0.95	0.73
	June 10a	1113	290.0	-1.7	2.2	0.93	0.91
	June 12a	1093	293.8	-2.7	3.3	0.67	0.63
	June 12b	1001	298.0	-1.7	2.2	0.90	0.85
	June 14a	1168	296.6	-1.7	2.3	0.73	0.75
	June 15a	1103	290.2	-1.1	2.2	0.05	0.42
	June 15b	1116	292.1	-3.8	5.1	0.94	0.82
	June 18a	1164	293.2	-0.2	2.5	0.93	0.96
	June 19a	1120	290.9	-2.3	3.2	0.90	0.83
	June 21a	1130	291.8	-2.0	2.8	-0.17	0.38
	June 21b	1126	296.6	-2.7	3.0	0.98	0.95
	June 23a	1180	292.6	-2.4	3.8	0.90	0.85
	June 23b	1106	296.1	-3.2	4.5	0.93	0.87
	June 24a	1173	292.3	1.4	3.6	-0.12	0.34
	June 24b	1034	294.7	-3.7	5.0	0.92	0.76
	June 27a	1215	298.7	-1.7	2.2	0.80	0.79
	June 28a	1139	301.3	-2.5	2.9	0.85	0.74
	June 28b	847	306.0	-0.9	2.3	0.88	0.89

Table S2. Performance of simulated relative humidity (RH) in terms of bias, RMSE, R, and IA for the individual G-1 aircraft flight paths.

Variable	Flight Date	Number of Data Points	Observed Mean	Bias	RMSE	R	IA
RH (%)	June 03a	849	60.2	7.2	10.9	0.22	0.47
	June 06a	1117	55.5	6.9	9.1	0.23	0.42
	June 06b	988	41.3	10.4	18.8	-0.20	0.23
	June 08a	1170	56.3	3.9	9.4	0.55	0.70
	June 08b	1212	40.1	-1.8	19.4	0.20	0.49
	June 10a	1111	38.9	1.2	12.0	0.18	0.51
	June 12a	1093	28.2	-1.8	5.3	-0.16	0.26
	June 12b	991	25.5	2.3	4.7	0.56	0.67
	June 14a	1168	32.2	2.6	9.6	0.54	0.70
	June 15a	1103	55.4	2.5	13.3	0.71	0.79
	June 15b	1115	42.4	-4.0	20.7	0.24	0.44
	June 18a	1142	25.2	-5.1	10.5	0.68	0.77
	June 19a	1097	39.3	2.7	11.8	0.35	0.60
	June 21a	1130	43.4	-5.1	8.2	0.56	0.65
	June 21b	1126	21.4	2.0	6.6	0.63	0.78
	June 23a	1180	40.5	-6.2	15.3	0.28	0.56
	June 23b	1077	30.5	0.7	14.4	-0.01	0.42
	June 24a	1173	44.3	-5.5	18.6	-0.08	0.35
	June 24b	1005	37.3	1.4	13.7	0.13	0.42
	June 27a	1215	41.4	-9.6	16.0	0.37	0.59
	June 28a	1136	38.3	2.2	7.9	0.51	0.71
	June 28b	843	25.2	-0.4	4.9	0.58	0.73

Table S3. Performance of simulated wind speed (WS) in terms of bias, RMSE, R, and IA for the individual G-1 aircraft flight paths.

Variable	Flight Date	Number of Data Points	Observed Mean	Bias	RMSE	R	IA
WS (m s^{-1})	June 03a	849	7.0	-1.3	3.3	-0.16	0.35
	June 06a	1117	3.5	-0.2	1.8	-0.01	0.36
	June 06b	989	6.1	-0.4	2.6	0.81	0.90
	June 08a	1170	3.8	-1.2	2.3	0.23	0.52
	June 08b	1213	5.3	-0.2	1.9	0.60	0.77
	June 10a	1112	8.0	0.5	1.8	0.55	0.70
	June 12a	1093	11.0	0.1	4.1	0.53	0.66
	June 12b	1001	9.8	-1.6	3.9	-0.15	0.27
	June 14a	1168	4.5	0.1	3.2	-0.23	0.27
	June 15a	1103	4.6	1.0	2.5	0.17	0.49
	June 15b	1115	5.5	0.8	2.6	0.54	0.70
	June 18a	1142	6.3	-2.0	3.6	0.23	0.50
	June 19a	1097	5.7	-0.5	2.1	-0.01	0.39
	June 21a	1130	4.5	2.7	4.3	0.60	0.66
	June 21b	1060	6.1	-2.0	12.3	0.06	0.11
	June 23a	1180	3.5	0.1	2.6	0.55	0.67
	June 23b	1077	3.9	0.8	2.6	0.35	0.56
	June 24a	1173	5.8	-2.0	3.4	0.37	0.57
	June 24b	1005	4.9	1.5	2.8	-0.06	0.32
	June 27a	1215	2.4	-0.2	1.9	-0.14	0.30
	June 28a	1136	2.8	-0.2	2.7	0.14	0.45
	June 28b	843	4.3	-1.2	2.4	-0.01	0.42

Table S4. Performance of simulated wind direction (WD) in terms of bias, RMSE, R, and IA for the individual G-1 aircraft flight paths.

Variable	Flight Date	Number of Data Points	Observed Mean	Bias	RMSE	R	IA
WD (°)	June 03a	849	225.0	31.1	41.3	0.41	0.50
	June 06a	1117	255.0	1.0	48.3	0.21	0.55
	June 06b	989	255.0	27.4	47.8	0.28	0.51
	June 08a	1170	165.0	45.8	83.7	0.31	0.64
	June 08b	1213	195.0	4.5	39.2	0.01	0.39
	June 10a	1112	315.0	-0.2	18.3	-0.03	0.55
	June 12a	1093	345.0	21.9	34.8	0.42	0.99
	June 12b	1001	315.0	15.6	26.7	0.08	0.75
	June 14a	1168	195.0	15.2	63.2	0.12	0.50
	June 15a	1103	195.0	4.9	40.4	0.61	0.79
	June 15b	1115	195.0	8.3	31.2	0.25	0.54
	June 18a	1142	315.0	16.2	51.8	0.71	0.78
	June 19a	1097	195.0	3.7	20.2	0.55	0.73
	June 21a	1130	345.0	2.2	62.8	0.57	0.83
	June 21b	1060	285.0	-6.4	40.5	0.07	0.89
	June 23a	1180	165.0	2.5	72.7	-0.11	0.69
	June 23b	1077	255.0	-0.4	53.8	0.17	0.49
	June 24a	1173	165.0	27.6	49.9	0.58	0.72
	June 24b	1005	165.0	-5.7	39.1	0.30	0.51
	June 27a	1215	285.0	12.2	100.3	-0.09	0.75
	June 28a	1136	255.0	-49.2	108.2	-0.12	0.59
	June 28b	843	255.0	45.1	70.5	-0.08	0.47

Table S5. Performance of simulated temperature (T) in terms of bias, RMSE, R, and IA for the individual WP-3D aircraft flight paths.

Variable	Flight Date	Number of Data Points	Observed Mean	Bias	RMSE	R	IA
T (K)	May 04	17219	287.5	-4.7	6.0	0.88	0.85
	May 07	24839	288.3	-5.5	6.4	0.90	0.84
	May 08	25439	286.6	-3.6	5.1	0.87	0.86
	May 11	25799	275.8	-5.2	6.1	0.97	0.95
	May 12	27489	285.1	-4.7	6.9	0.91	0.89
	May 14	22259	285.6	-0.4	3.9	0.87	0.93
	May 16	27899	286.5	-2.8	4.4	0.87	0.89
	May 19	24239	287.0	-3.2	4.8	0.86	0.87
	May 21	10722	286.8	0.4	1.5	0.82	0.89
	May 24	22619	283.4	-1.2	2.5	0.98	0.98
	May 30	20879	293.5	-0.7	2.3	0.87	0.92
	May 31	21278	292.3	-0.2	3.8	0.75	0.85
	June 02	22259	287.1	0.8	2.8	0.71	0.82
	June 03	24179	290.8	0.0	4.0	0.70	0.77
	June 14	26459	289.0	-3.5	4.5	0.97	0.97
	June 16	24899	289.7	-3.3	4.8	0.84	0.85
	June 18	25499	288.6	-2.0	3.6	0.88	0.91
	June 20	25619	290.6	-3.2	4.9	0.70	0.76
	June 22	22679	287.3	-9.6	10.1	0.92	0.74

Table S6. Performance of simulated relative humidity (RH) in terms of bias, RMSE, R, and IA for the individual WP-3D aircraft flight paths.

Variable	Flight Date	Number of Data Points	Observed Mean	Bias	RMSE	R	IA
RH (%)	May 04	17219	22.5	-7.4	13.6	0.72	0.73
	May 07	24839	25.8	4.3	12.1	0.18	0.49
	May 08	25439	30.2	-0.9	15.1	0.72	0.83
	May 11	25799	39.4	6.5	19.2	0.67	0.79
	May 12	27489	41.6	1.4	21.4	0.51	0.71
	May 14	22259	49.3	-10.6	24.8	0.50	0.61
	May 16	27899	51.9	-6.2	19.4	0.81	0.89
	May 19	24239	44.2	-14.6	21.3	0.58	0.64
	May 21	10722	40.5	-6.4	17.5	0.83	0.90
	May 24	22619	39.5	-6.6	16.3	0.36	0.59
	May 30	20879	21.7	-4.0	11.7	0.78	0.76
	May 31	21278	27.3	-10.1	19.9	0.57	0.58
	June 02	22259	59.6	-12.2	20.2	0.41	0.57
	June 03	24179	51.2	-8.7	18.6	0.73	0.64
	June 14	26459	30.1	5.3	13.8	0.70	0.82
	June 16	24899	38.1	-1.6	18.2	0.70	0.83
	June 18	25499	41.5	0.3	14.7	0.84	0.92
	June 20	25619	35.6	-10.1	17.4	0.82	0.81
	June 22	22679	16.8	-0.7	8.8	0.18	0.47

Table S7. Performance of wind speed (WS) in terms of bias, RMSE, R, and IA for the individual WP-3D aircraft flight paths.

Variable	Flight Date	Number of Data Points	Observed Mean	Bias	RMSE	R	IA
WS (m s^{-1})	May 04	17219	4.9	1.5	3.3	0.35	0.61
	May 07	24839	4.5	0.5	2.6	0.81	0.89
	May 08	25439	7.9	0.1	3.6	0.76	0.87
	May 11	25799	11.0	2.3	7.6	0.85	0.86
	May 12	25289	7.3	0.3	6.3	0.49	0.62
	May 14	22259	3.1	-0.3	2.3	0.23	0.55
	May 16	27899	5.1	-1.7	3.1	0.44	0.60
	May 19	24239	8.4	-1.4	4.8	0.67	0.79
	May 21	10722	10.4	1.6	3.9	0.83	0.90
	May 24	22619	6.2	-1.7	3.1	0.61	0.70
	May 30	20879	5.5	0.2	3.6	0.11	0.45
	May 31	21278	4.1	1.1	3.8	0.11	0.48
	June 02	22259	3.4	1.1	3.7	0.13	0.47
	June 03	24179	3.3	0.5	2.7	0.39	0.62
	June 14	26459	7.4	-1.7	3.3	0.73	0.81
	June 16	24899	7.6	-0.3	3.1	0.79	0.88
	June 18	25499	7.8	-1.8	3.8	0.75	0.83
	June 20	25619	4.8	0.4	2.6	0.64	0.79
	June 22	22679	6.5	-1.9	3.8	0.70	0.77
	June 20	25619	255.0	24.4	70.5	0.34	0.61
	June 22	22679	225.0	14.4	65.7	0.30	0.78

Table S8. Performance of wind direction (WD) in terms of bias, RMSE, R, and IA for the individual WP-3D aircraft flight paths.

Variable	Flight Date	Number of Data Points	Observed Mean	Bias	RMSE	R	IA
WD (°)	May 04	17219	285.0	7.5	53.1	0.09	0.57
	May 07	24839	345.0	-10.3	76.4	0.16	0.81
	May 08	25439	255.0	-1.7	53.4	0.20	0.49
	May 11	25799	345.0	1.3	40.1	0.11	0.85
	May 12	25289	315.0	-2.4	62.4	0.04	0.48
	May 14	22259	255.0	20.6	99.2	-0.11	0.73
	May 16	27899	285.0	-24.6	95.2	-0.02	0.57
	May 19	24239	345.0	1.9	74.8	0.29	0.68
	May 21	10722	315.0	-1.1	35.0	0.26	0.52
	May 24	22619	315.0	-24.1	38.0	0.34	0.64
	May 30	20879	285.0	-2.1	66.1	0.42	0.90
	May 31	21278	315.0	-18.1	87.3	0.12	0.70
	June 02	22259	285.0	-11.8	84.2	0.23	0.84
	June 03	24179	345.0	-10.1	84.3	0.17	0.84
	June 14	26459	255.0	-16.8	57.6	0.51	0.84
	June 16	24899	315.0	-7.5	39.2	0.28	0.80
	June 18	25499	255.0	-3.2	47.0	0.57	0.83

Table S9. Performance of simulated temperature (T) in terms of bias, RMSE, R, and IA for the individual CIRPAS Twin Otter aircraft flight paths.

Variable	Flight Date	Number of Data Points	Observed Mean	Bias	RMSE	R	IA
T (K)	May 04	187	293.7	-2.3	3.5	0.14	0.40
	May 05	228	291.8	-2.0	3.6	-0.09	0.33
	May 06	179	290.0	-2.0	2.6	0.17	0.46
	May 07	194	294.9	-3.6	5.0	0.09	0.32
	May 10	182	286.7	-1.1	2.4	0.48	0.54
	May 12	195	291.9	-4.8	5.5	0.67	0.54
	May 13	174	294.3	-2.3	3.6	0.76	0.80
	May 14	189	289.5	0.4	1.5	0.68	0.77
	May 15	185	292.2	-1.7	2.7	0.72	0.74
	May 18	183	283.6	-2.5	3.5	0.96	0.93
	May 19	192	290.6	-1.1	2.1	0.37	0.54
	May 20	192	288.0	-4.6	5.3	0.85	0.74
	May 21	192	288.7	-2.4	3.0	0.58	0.63
	May 22	195	279.1	-4.3	4.7	0.95	0.87
	May 24	189	285.8	-5.7	6.7	0.87	0.76
	May 25	191	289.8	-5.7	6.5	0.81	0.63
	May 27	176	287.9	-3.4	4.1	0.28	0.32
	May 28	192	288.1	-4.2	4.7	0.38	0.27

Table S10. Performance of simulated relative humidity (RH) in terms of bias, RMSE, R, and IA for the individual CIRPAS Twin Otter aircraft flight paths.

Variable	Flight Date	Number of Data Points	Observed Mean	Bias	RMSE	R	IA
RH (%)	May 04	187	40.1	-10.1	12.1	0.87	0.78
	May 05	228	51.9	-16.2	19.0	0.78	0.67
	May 06	178	57.4	-17.2	41.4	0.29	0.37
	May 07	194	36.0	-9.3	20.8	0.57	0.61
	May 10	182	61.6	4.8	13.0	-0.12	0.27
	May 12	195	35.9	6.7	11.7	0.85	0.88
	May 13	174	31.8	-3.6	10.1	0.79	0.82
	May 14	189	65.1	-18.2	22.2	0.67	0.55
	May 15	185	57.3	-12.7	18.3	0.71	0.75
	May 18	183	48.5	-1.8	14.6	0.90	0.90
	May 19	192	64.8	-18.2	21.9	0.62	0.51
	May 20	192	38.9	6.4	22.5	0.78	0.82
	May 21	192	64.3	-18.5	26.4	0.56	0.63
	May 22	194	38.2	1.7	25.9	0.46	0.68
	May 24	189	35.9	4.2	13.0	0.73	0.85
	May 25	191	38.5	0.1	11.1	0.72	0.85
	May 27	176	66.1	7.3	15.6	-0.29	0.13
	May 28	192	54.9	-6.9	12.4	0.68	0.68

Table S11. Performance of simulated temperature (T) in terms of bias, RMSE, R, and IA for the R/V Atlantis paths by day.

Variable	Flight Date	Number of Data Points	Observed Mean	Bias	RMSE	R	IA
T (K)	May 14	359	287.6	-1.9	2.0	0.03	0.17
	May 15	1409	286.6	0.6	1.3	-0.43	0.11
	May 16	1424	285.9	1.6	1.7	0.25	0.35
	May 17	1433	285.0	0.8	1.0	0.12	0.46
	May 18	1413	285.7	0.7	1.0	0.35	0.53
	May 19	1427	286.8	0.5	0.9	-0.57	0.31
	May 20	1439	288.0	-0.1	1.9	0.43	0.62
	May 21	1433	288.1	1.6	2.7	-0.23	0.12
	May 22	1417	288.4	1.5	2.1	0.12	0.47
	May 23	1440	286.1	1.1	1.3	0.48	0.51
	May 24	1429	286.2	0.7	0.9	-0.07	0.44
	May 25	1440	286.0	0.9	1.2	-0.17	0.44
	May 26	1440	288.2	-0.5	1.1	0.90	0.89
	May 27	1440	288.6	0.4	1.4	0.51	0.70
	May 28	1440	287.8	0.8	1.5	0.46	0.59
	May 29	1440	287.5	0.6	1.4	0.24	0.45
	May 30	1434	288.9	1.6	3.3	0.11	0.34
	May 31	1432	287.1	3.7	4.8	-0.18	0.12
	June 01	1440	285.1	1.6	1.7	0.67	0.45
	June 02	1440	285.0	0.5	1.4	0.29	0.48
	June 03	1440	291.2	3.8	4.5	0.79	0.74
	June 04	1440	293.4	0.2	2.8	-0.30	0.12
	June 05	1440	294.1	-2.3	5.2	-0.66	0.31
	June 06	1440	290.6	5.1	6.7	0.66	0.55
	June 07	1440	285.9	0.6	1.3	0.87	0.86
	June 08	720	285.8	1.8	2.1	0.84	0.41

Table S12. Performance of simulated relative humidity (RH) in terms of bias, RMSE, R, and IA for the R/V Atlantis paths by day.

Variable	Flight Date	Number of Data Points	Observed Mean	Bias	RMSE	R	IA
RH (%)	May 14	359	79.7	14.5	14.6	0.14	0.12
	May 15	1409	88.2	2.4	6.4	-0.07	0.33
	May 16	1424	92.8	-2.3	3.8	-0.05	0.40
	May 17	1433	94.7	-2.3	4.4	0.46	0.56
	May 18	1413	94.8	-1.6	3.0	0.06	0.42
	May 19	1427	94.3	-3.8	4.7	-0.11	0.37
	May 20	1439	91.4	-4.3	13.4	0.35	0.46
	May 21	1433	83.5	-13.2	17.7	-0.11	0.21
	May 22	1417	71.3	-7.8	11.5	0.27	0.53
	May 23	1440	67.5	3.6	5.4	0.84	0.86
	May 24	1429	80.0	-3.4	4.7	0.58	0.57
	May 25	1440	85.0	-9.2	12.5	-0.52	0.20
	May 26	1440	81.2	2.1	5.8	0.90	0.94
	May 27	1440	76.2	-1.7	9.6	0.63	0.79
	May 28	1440	78.4	-13.8	16.8	0.67	0.51
	May 29	1440	84.4	-10.3	13.9	0.03	0.30
	May 30	1434	86.4	-20.6	28.3	0.22	0.46
	May 31	1432	91.7	-29.9	33.3	-0.13	0.09
	June 01	1440	95.9	-3.2	8.8	0.14	0.35
	June 02	1440	93.1	-8.8	11.6	0.41	0.53
	June 03	1440	79.1	-9.0	14.6	0.71	0.74
	June 04	1440	71.3	-3.5	14.6	-0.11	0.29
	June 05	1440	74.0	6.3	23.2	-0.68	0.20
	June 06	1440	84.1	-28.0	32.2	0.59	0.51
	June 07	1440	95.6	1.5	2.8	0.95	0.97
	June 08	720	89.2	-10.3	11.2	0.91	0.37

Table S13. Performance of simulated wind speed (WS) in terms of bias, RMSE, R, and IA for the R/V Atlantis paths by day.

Variable	Flight Date	Number of Data Points	Observed Mean	Bias	RMSE	R	IA
WS (ms^{-1})	May 14	359	4.4	-1.0	1.3	0.42	0.48
	May 15	1408	3.3	0.4	2.0	0.15	0.41
	May 16	1424	3.6	1.8	2.6	0.46	0.56
	May 17	1433	2.8	0.2	2.6	-0.31	0.23
	May 18	1413	4.4	-2.7	3.6	0.45	0.50
	May 19	1427	5.2	1.0	2.6	0.01	0.43
	May 20	1439	4.3	1.4	2.6	0.02	0.43
	May 21	1433	4.5	4.4	5.8	-0.05	0.34
	May 22	1417	2.8	4.4	4.9	0.84	0.53
	May 23	1440	9.6	2.5	4.1	0.34	0.49
	May 24	1429	5.9	7.8	8.8	-0.71	0.34
	May 25	1440	4.7	3.8	5.6	-0.07	0.40
	May 26	1440	4.4	3.0	3.6	0.26	0.47
	May 27	1440	2.6	3.1	3.4	-0.28	0.33
	May 28	1440	5.4	3.8	4.5	0.31	0.46
	May 29	1440	3.7	6.1	6.7	-0.22	0.28
	May 30	1434	4.3	3.5	4.5	0.14	0.45
	May 31	1432	2.9	0.5	3.2	0.35	0.41
	June 01	1440	7.9	2.0	4.3	0.41	0.63
	June 02	1440	4.4	6.3	8.5	-0.20	0.35
	June 03	1440	5.6	0.8	2.3	0.28	0.49
	June 04	1440	4.8	-0.5	1.5	0.12	0.33
	June 05	1440	3.3	-1.8	2.4	0.84	0.59
	June 06	1440	6.5	-0.5	2.1	0.01	0.38
	June 07	1440	10.9	-2.2	3.4	0.47	0.56
	June 08	720	5.7	3.5	4.1	0.35	0.41

Table S14. Performance of simulated wind direction (WD) in terms of bias, RMSE, R, and IA for the R/V Atlantis paths by day.

Variable	Flight Date	Number of Data Points	Observed Mean	Bias	RMSE	R	IA
WD (°)	May 14	359	225.0	-9.0	29.7	-0.45	0.21
	May 15	1408	255.0	0.4	65.5	-0.09	0.43
	May 16	1424	195.0	41.0	90.4	0.25	0.52
	May 17	1433	255.0	-40.7	99.6	-0.36	0.20
	May 18	1413	105.0	65.4	129.3	0.46	0.54
	May 19	1427	255.0	19.1	29.2	0.47	0.51
	May 20	1439	225.0	51.0	73.3	0.22	0.52
	May 21	1433	225.0	-9.3	71.1	0.43	0.60
	May 22	1417	255.0	22.9	55.4	0.20	0.44
	May 23	1440	285.0	5.2	16.8	0.32	0.51
	May 24	1429	255.0	16.2	104.1	0.82	0.63
	May 25	1440	285.0	16.7	80.7	0.43	0.55
	May 26	1440	285.0	17.0	57.4	-0.25	0.45
	May 27	1440	285.0	9.9	87.1	0.26	0.52
	May 28	1440	285.0	13.0	63.0	-0.41	0.41
	May 29	1440	255.0	-17.6	82.6	-0.50	0.73
	May 30	1434	105.0	-18.7	118.2	-0.20	0.60
	May 31	1432	315.0	32.6	91.8	0.46	0.58
	June 01	1440	315.0	-7.4	39.1	0.67	0.72
	June 02	1440	285.0	19.3	77.1	0.16	0.53
	June 03	1440	225.0	18.5	35.8	0.19	0.48
	June 04	1440	195.0	18.6	32.1	0.24	0.45
	June 05	1440	135.0	-5.5	54.6	0.52	0.70
	June 06	1440	285.0	14.9	25.6	0.80	0.78
	June 07	1440	315.0	11.4	24.3	0.89	0.77
	June 08	720	225.0	31.9	35.7	-0.03	0.38

Table S15. Performance of simulated carbon monoxide (CO), the sum of nitrogen oxide and nitrogen dioxide (NO_x), sulfur dioxide (SO_2), and ozone (O_3), from the DEF_ANT simulation in terms of bias, RMSE, R, and IA relative to observations at the four supersites (Fig. 1a,b) and the surface operational air quality sampling stations depicted in Fig. 1d. Statistics given for all of California (CA) and by regions as shown in Fig. 1c.

Table S15. (continued).

Variables	Regions and Supersites	Observed	Mean	Bias	RMSE	R	IA
CO (ppbv)	CA	269.9	260.0	-2.0	0.14	0.39	
	Southern CA	319.8	298.4	1.3	0.03	0.35	
	San Joaquin	172.9	115.2	31.2	0.20	0.45	
	Sacramento Valley	201.6	98.0	4.8	0.20	0.45	
	Coastal	206.2	143.2	-25.0	0.24	0.48	
	Interior Mountains	249.0	424.0	-59.3	0.07	0.11	
	Bakersfield	166.7	81.3	48.1	0.47	0.50	
	Pasadena	306.6	291.9	225.6	0.45	0.36	
	T0	154.5	129.1	79.5	0.23	0.38	
	T1	122.8	86.0	69.1	0.31	0.33	
NO _x (ppbv)	CA	9.7	22.4	6.2	0.33	0.46	
	Southern CA	13.1	29.7	9.1	0.24	0.40	
	San Joaquin	8.3	15.8	5.8	0.52	0.55	
	Sacramento Valley	6.2	13.1	6.5	0.36	0.42	
	Coastal	4.5	8.9	2.4	0.36	0.52	
	Interior Mountains	8.5	10.8	-2.0	0.23	0.43	
	Bakersfield	—	—	—	—	—	
	Pasadena	16.3	50.5	40.8	0.45	0.27	
	T0	7.0	14.7	8.3	0.25	0.34	
	T1	—	—	—	—	—	
SO ₂ (ppbv)	CA	0.8	3.5	0.9	0.05	0.17	
	Southern CA	0.9	4.4	1.4	0.03	0.14	
	San Joaquin	1.3	1.1	-0.3	0.14	0.45	
	Sacramento Valley	0.7	1.2	0.3	0.47	0.64	
	Coastal	0.4	2.5	0.7	-0.07	0.12	
	Interior Mountains	0.9	1.7	-0.5	0.04	0.30	
	Bakersfield	0.8	1.0	0.0	-0.21	0.24	
	Pasadena	0.3	2.0	1.4	0.05	0.14	
	T0	0.4	0.9	0.4	0.32	0.47	
	T1	—	—	—	—	—	
O ₃ (ppbv)	CA	36.6	13.9	-3.9	0.71	0.83	
	Southern CA	38.5	15.9	-2.8	0.65	0.80	
	San Joaquin	38.7	14.0	-8.6	0.84	0.86	
	Sacramento Valley	30.4	12.5	-6.1	0.77	0.83	
	Coastal	29.5	11.4	-2.2	0.61	0.77	
	Interior Mountains	42.4	11.8	-3.7	0.73	0.84	
	Bakersfield	39.1	17.8	-13.2	0.84	0.83	
	Pasadena	33.1	20.4	-14.8	0.68	0.70	
	T0	32.1	13.5	-8.0	0.86	0.87	
	T1	39.7	13.0	-5.4	0.76	0.84	

Table S16. Same as Table S15, except from 50%_ANT simulation.

Variable	Regions and Supersites	Observed	Mean	Bias	RMSE	R	IA
CO (ppbv)	CA	269.9	269.9	-71.9	243.7	0.17	0.37
	Southern CA	319.8	319.8	-92.5	273.5	0.07	0.38
	San Joaquin	172.9	172.9	-10.3	106.0	0.20	0.35
	Sacramento Valley	201.6	201.6	-37.3	89.4	0.21	0.44
	Coastal	206.2	206.2	-56.6	146.6	0.25	0.45
	Interior Mountains	249.0	249.0	-92.9	429.3	0.05	0.13
	Bakersfield	166.7	166.7	-0.9	39.8	0.49	0.69
	Pasadena	306.6	306.6	24.6	105.6	0.43	0.63
	T0	154.5	154.5	18.9	72.0	0.26	0.46
	T1	122.8	122.8	32.1	45.5	0.27	0.46
NO _x (ppbv)	CA	9.74	9.74	-2.05	13.4	0.33	0.56
	Southern CA	13.1	13.1	-2.45	17.6	0.24	0.51
	San Joaquin	8.30	8.30	-1.42	8.1	0.53	0.70
	Sacramento Valley	6.16	6.16	-0.02	6.5	0.37	0.58
	Coastal	4.51	4.51	-1.09	6.0	0.36	0.57
	Interior Mountains	8.49	8.49	-5.41	11.4	0.24	0.36
	Bakersfield	—	—	—	—	—	—
	Pasadena	16.3	16.3	11.03	17.9	0.47	0.53
	T0	7.00	7.00	0.36	7.3	0.26	0.47
	T1	—	—	—	—	—	—
SO ₂ (ppbv)	CA	0.77	0.77	0.88	3.5	0.05	0.17
	Southern CA	0.88	0.88	1.35	4.4	0.03	0.14
	San Joaquin	1.28	1.28	-0.34	1.1	0.15	0.46
	Sacramento Valley	0.72	0.72	0.30	1.2	0.46	0.64
	Coastal	0.41	0.41	0.71	2.5	-0.07	0.13
	Interior Mountains	0.86	0.86	-0.53	1.7	0.04	0.30
	Bakersfield	0.79	0.79	0.00	1.0	-0.21	0.24
	Pasadena	0.32	0.32	1.34	2.0	0.05	0.14
	T0	0.38	0.38	0.42	0.9	0.33	0.48
	T1	—	—	—	—	—	—
O ₃ (ppbv)	CA	36.6	36.6	-4.0	13.1	0.70	0.81
	Southern CA	38.5	38.5	-1.7	14.9	0.63	0.79
	San Joaquin	38.7	38.7	-8.9	13.0	0.83	0.85
	Sacramento Valley	30.4	30.4	-5.5	10.7	0.78	0.84
	Coastal	29.5	29.5	-2.6	10.5	0.61	0.77
	Interior Mountains	42.4	42.4	-6.8	12.4	0.73	0.79
	Bakersfield	39.1	39.1	-12.2	16.0	0.85	0.83
	Pasadena	33.1	33.1	-8.4	16.9	0.66	0.77
	T0	32.1	32.1	-7.0	11.6	0.85	0.88
	T1	39.7	39.7	-9.1	13.2	0.77	0.80

Table S17. Same as Table S15, except from 0%_ANT simulation.

Variable	Regions and Supersites	Observed	Mean	Bias	RMSE	R	IA
CO (ppbv)	CA	269.9	268.2	-140.2	0.19	0.37	
	Southern CA	319.8	304.8	-183.9	0.17	0.40	
	San Joaquin	172.9	118.1	-51.3	0.13	0.39	
	Sacramento Valley	201.6	112.7	-79.0	0.05	0.39	
	Coastal	206.2	164.0	-87.5	0.11	0.42	
	Interior Mountains	249.0	438.7	-125.7	-0.03	0.15	
	Bakersfield	166.7	62.8	-49.6	0.27	0.43	
	Pasadena	306.6	194.8	-171.9	-0.05	0.37	
	T0	154.5	74.7	-41.3	0.33	0.39	
	T1	122.8	28.3	-5.1	-0.16	0.26	
NO _x (ppbv)	CA	9.74	15.2	-9.57	0.18	0.38	
	Southern CA	13.1	19.4	-12.94	0.13	0.39	
	San Joaquin	8.30	11.2	-8.11	0.39	0.39	
	Sacramento Valley	6.16	8.2	-5.96	0.32	0.39	
	Coastal	4.51	7.3	-4.42	0.21	0.38	
	Interior Mountains	8.49	13.3	-8.36	0.06	0.36	
	Bakersfield	—	—	—	—	—	
	Pasadena	16.3	18.7	-16.1	-0.10	0.38	
	T0	7.00	9.1	-6.77	0.37	0.38	
	T1	—	—	—	—	—	
SO ₂ (ppbv)	CA	0.77	1.2	-0.70	0.04	0.40	
	Southern CA	0.88	1.3	-0.76	0.01	0.40	
	San Joaquin	1.28	1.5	-1.28	-0.04	0.39	
	Sacramento Valley	0.72	1.2	-0.71	-0.01	0.43	
	Coastal	0.41	0.7	-0.41	0.01	0.47	
	Interior Mountains	0.86	1.8	-0.85	-0.02	0.35	
	Bakersfield	0.79	1.0	-0.79	-0.15	0.42	
	Pasadena	0.32	0.4	-0.24	-0.12	0.37	
	T0	0.38	0.7	-0.37	0.05	0.35	
	T1	—	—	—	—	—	
O ₃ (ppbv)	CA	36.6	18.6	-9.8	0.39	0.57	
	Southern CA	38.5	20.7	-8.1	0.24	0.50	
	San Joaquin	38.7	19.9	-14.8	0.60	0.59	
	Sacramento Valley	30.4	13.5	-8.2	0.60	0.68	
	Coastal	29.5	12.5	-6.2	0.48	0.62	
	Interior Mountains	42.4	20.6	-15.5	0.44	0.54	
	Bakersfield	39.1	22.6	-16.4	0.67	0.59	
	Pasadena	33.1	20.2	-5.4	0.26	0.53	
	T0	32.1	17.3	-12.2	0.67	0.63	
	T1	39.7	23.5	-19.9	0.52	0.51	

Table S18. Performance of simulated carbon monoxide (CO) from the DEF_ANT simulation in terms of bias, RMSE, R, and IA for each for the G-1 flights.

Variable	Flight Date	Number of Data Points	Observed Mean	Bias	RMSE	R	IA
	June 03a	800	129.7	0.8	14.8	0.12	0.44
	June 06a	1097	120.6	11.8	20.3	0.81	0.76
	June 06b	943	124.8	-2.1	16.8	0.31	0.59
	June 08a	1142	156.1	-7.1	20.2	0.54	0.71
	June 08b	1147	149.0	7.9	28.6	0.71	0.69
	June 10a	1068	126.3	-5.0	9.3	0.18	0.43
	June 12a	1042	113.2	10.6	16.7	0.13	0.33
	June 12b	950	127.7	4.5	10.6	0.03	0.41
	June 14a	1120	164.7	5.3	35.1	0.36	0.60
	June 15a	1055	144.9	32.7	37.5	0.73	0.49
CO (ppbv)	June 15b	1071	150.5	25.3	35.1	0.29	0.44
	June 18a	1114	132.9	-2.6	24.4	0.39	0.58
	June 19a	1050	135.3	27.6	31.6	0.41	0.36
	June 21a	1077	134.6	14.9	25.3	0.54	0.63
	June 21b	1043	128.0	18.0	26.0	0.39	0.48
	June 23a	1012	171.8	3.6	49.8	-0.16	0.27
	June 23b	1003	157.3	27.6	42.0	0.24	0.42
	June 24a	1122	110.4	25.1	57.7	-0.37	0.26
	June 24b	922	120.8	17.5	42.7	0.35	0.52
	June 27a	1163	147.4	42.6	62.2	0.36	0.49
	June 28a	1051	166.3	54.0	78.7	0.65	0.64
	June 28b	750	155.7	0.6	24.2	0.54	0.71

Table S19. Performance of simulated nitrogen oxide (NO) from the DEF_ANT simulation in terms of bias, RMSE, R, and IA for each for the G-1 flights.

Variable	Flight Date	Number of Data Points	Observed Mean	Bias	RMSE	R	IA
	June 03a	816	0.3	0.4	0.9	0.59	0.52
	June 06a	1069	0.2	0.6	1.2	0.85	0.48
	June 06b	946	0.1	0.0	0.2	0.14	0.42
	June 08a	1119	1.0	0.4	1.5	0.65	0.73
	June 08b	—	—	—	—	—	—
	June 10a	1066	0.2	0.1	0.2	0.38	0.57
	June 12a	1048	0.2	0.0	0.2	0.64	0.80
	June 12b	952	0.2	0.0	0.1	0.28	0.53
	June 14a	1117	1.0	0.4	2.0	0.17	0.40
	June 15a	1054	1.0	1.8	2.7	0.80	0.58
NO (ppbv)	June 15b	1067	0.2	0.1	0.2	0.54	0.69
	June 18a	1097	0.2	0.0	0.3	0.49	0.65
	June 19a	995	0.2	0.0	0.1	0.70	0.81
	June 21a	1080	0.8	0.5	1.4	0.32	0.53
	June 21b	1045	0.2	0.1	0.3	0.20	0.40
	June 23a	1129	0.4	0.1	0.9	0.67	0.79
	June 23b	975	0.2	0.0	0.2	0.49	0.66
	June 24a	1083	1.1	0.2	1.9	0.32	0.55
	June 24b	899	0.4	0.6	1.2	0.74	0.49
	June 27a	1131	0.1	0.2	0.5	0.64	0.52
	June 28a	1054	0.5	1.1	2.6	0.29	0.28
	June 28b	749	0.2	0.0	0.1	0.25	0.50

Table S20. Performance of simulated nitrogen dioxide (NO_2) from the DEF_ANT simulation in terms of bias, RMSE, R, and IA for each for the G-1 flights.

Variable	Flight Date	Number of Data Points	Observed Mean	Bias	RMSE	R	IA
NO_2 (ppbv)	June 03a	777	0.7	0.2	0.8	0.66	0.72
	June 06a	1016	0.6	0.7	1.3	0.84	0.61
	June 06b	899	0.4	0.1	0.4	0.45	0.59
	June 08a	1061	2.2	-0.4	1.6	0.67	0.79
	June 08b	—	—	—	—	—	—
	June 10a	965	0.6	0.1	0.3	0.42	0.60
	June 12a	995	0.4	0.0	0.3	0.73	0.84
	June 12b	900	0.5	0.1	0.3	0.53	0.64
	June 14a	1060	2.2	1.2	3.4	0.33	0.51
	June 15a	1003	1.7	2.3	3.0	0.81	0.60
	June 15b	1009	0.9	0.5	1.0	0.46	0.60
	June 18a	1042	0.9	0.0	0.9	0.66	0.76
	June 19a	948	0.0	0.9	1.1	-0.27	0.03
	June 21a	1024	1.8	0.5	1.8	0.46	0.65
	June 21b	991	0.7	0.5	1.3	0.34	0.36
	June 23a	1072	0.9	0.3	1.6	0.73	0.80
	June 23b	928	0.9	0.4	0.9	0.61	0.66
	June 24a	1027	1.7	0.0	2.0	0.41	0.65
	June 24b	856	1.1	1.3	2.5	0.74	0.56
	June 27a	1078	0.5	0.7	1.4	0.62	0.46
	June 28a	1001	2.0	3.2	6.4	0.50	0.48
	June 28b	709	1.0	0.2	0.6	0.40	0.62

Table S21. Performance of simulated sulfur dioxide (SO_2) from the DEF_ANT simulation in terms of bias, RMSE, R, and IA for each for the G-1 flights.

Variable	Flight Date	Number of Data Points	Observed Mean	Bias	RMSE	R	IA
SO_2 (ppbv)	June 03a	808	-0.3	0.5	1.0	-0.08	0.34
	June 06a	1048	0.2	-0.1	0.8	0.11	0.22
	June 06b	941	-0.1	0.2	0.8	0.00	0.23
	June 08a	—	—	—	—	—	—
	June 08b	—	—	—	—	—	—
	June 10a	—	—	—	—	—	—
	June 12a	—	—	—	—	—	—
	June 12b	—	—	—	—	—	—
	June 14a	—	—	—	—	—	—
	June 15a	1037	0.8	0.0	0.4	0.69	0.82
	June 15b	1046	0.8	-0.4	0.7	0.31	0.53
	June 18a	1082	0.8	-0.7	1.1	0.13	0.43
	June 19a	1028	0.7	-0.3	0.5	0.51	0.63
	June 21a	1071	0.6	-0.3	0.8	0.11	0.43
	June 21b	1037	0.5	-0.2	0.6	0.40	0.60
	June 23a	1112	0.7	-0.4	0.6	0.41	0.53
	June 23b	955	1.0	-0.7	0.9	0.39	0.46
	June 24a	944	0.5	0.1	0.9	0.19	0.44
	June 24b	889	1.0	-0.7	0.9	0.30	0.49
	June 27a	1093	0.6	-0.1	0.6	0.50	0.55
	June 28a	1031	0.9	-0.6	1.0	0.10	0.45
	June 28b	722	0.6	-0.5	0.8	0.29	0.44

Table S22. Performance of simulated ozone (O_3) from the DEF_ANT simulation in terms of bias, RMSE, R, and IA for each for the G-1 flights.

Variable	Flight Date	Number of Data Points	Observed Mean	Bias	RMSE	R	IA
O_3 (ppbv)	June 03a	835	38.2	-9.2	10.7	0.55	0.54
	June 06a	1132	29.0	-1.8	6.8	0.48	0.70
	June 06b	969	48.9	-10.3	17.9	-0.07	0.32
	June 08a	1152	44.0	-5.0	10.8	0.83	0.85
	June 08b	1194	60.2	-3.2	7.3	0.79	0.86
	June 10a	1088	43.5	-4.7	5.7	0.51	0.51
	June 12a	1078	37.2	5.3	5.8	0.80	0.57
	June 12b	—	—	—	—	—	—
	June 14a	1075	44.9	6.8	9.8	0.49	0.58
	June 15a	1065	36.4	-1.2	5.8	0.81	0.89
	June 15b	1082	63.5	6.1	9.6	0.09	0.36
	June 18a	1145	52.1	1.0	8.6	0.64	0.80
	June 19a	1101	49.1	7.7	10.3	0.28	0.36
	June 21a	1128	34.8	0.8	5.5	0.61	0.77
	June 21b	1035	55.9	4.7	9.2	0.02	0.40
	June 23a	1167	58.5	7.2	10.9	0.81	0.83
	June 23b	1024	71.5	18.4	20.8	0.39	0.35
	June 24a	1125	32.2	6.0	14.2	0.59	0.66
	June 24b	951	44.5	1.1	7.2	0.52	0.69
	June 27a	1152	48.5	18.0	21.2	0.26	0.29
	June 28a	1121	55.4	11.4	21.5	0.34	0.56
	June 28b	759	65.6	10.4	17.7	0.53	0.66

Table S23. Performance of simulated isoprene from the DEF_ANT simulation in terms of bias, RMSE, R, and IA for each for the G-1 flights.

Variable	Flight Date	Number of Data Points	Observed Mean	Bias	RMSE	R	IA
isoprene (ppbv)	June 03a	854	-0.2	0.2	0.3	0.71	0.44
	June 06a	1133	0.4	-0.3	0.6	0.61	0.52
	June 06b	705	0.1	-0.1	0.2	0.25	0.46
	June 08a	1190	0.4	-0.3	0.5	0.61	0.47
	June 08b	1140	0.0	0.0	0.4	0.34	0.19
	June 10a	1113	0.1	0.0	0.1	0.47	0.61
	June 12a	1114	0.2	-0.1	0.2	0.69	0.81
	June 12b	—	—	—	—	—	—
	June 14a	1168	0.3	-0.1	0.4	0.25	0.43
	June 15a	1110	0.3	-0.2	0.3	0.41	0.55
	June 15b	1115	0.5	-0.4	0.6	0.47	0.51
	June 18a	632	0.2	-0.1	0.6	0.17	0.13
	June 19a	1071	1.0	-0.8	0.9	0.28	0.28
	June 21a	1075	0.4	-0.3	0.3	0.53	0.52
	June 21b	1126	0.4	-0.3	0.4	0.57	0.47
	June 23a	1079	0.6	-0.4	0.7	0.73	0.64
	June 23b	1106	1.2	-1.1	1.5	0.32	0.47
	June 24a	1173	0.3	-0.3	0.5	-0.09	0.33
	June 24b	1034	0.8	-0.7	1.1	-0.07	0.45
	June 27a	840	1.6	-1.2	2.3	0.83	0.54
	June 28a	1105	1.5	-1.2	2.3	0.76	0.51
	June 28b	755	1.1	-0.9	1.4	0.61	0.48

Table S24. Performance of simulated methyl-vinyl-ketone + methacrolein (MVK+MACR) from the DEF_ANT simulation in terms of bias, RMSE, R, and IA for each for the G-1 flights.

Variable	Flight Date	Number of Data Points	Observed Mean	Bias	RMSE	R	IA
MVK+ MACR (ppbv)	June 03a	854	0.0	0.0	0.1	0.68	0.59
	June 06a	1133	0.4	-0.2	0.3	0.72	0.67
	June 06b	705	0.2	0.0	0.1	0.65	0.76
	June 08a	1190	0.4	-0.2	0.4	0.62	0.56
	June 08b	1140	0.7	-0.6	0.7	0.52	0.50
	June 10a	1113	0.1	-0.1	0.1	0.72	0.73
	June 12a	1114	0.2	0.0	0.1	0.60	0.75
	June 12b	—	—	—	—	—	—
	June 14a	1168	0.4	-0.1	0.3	0.39	0.54
	June 15a	1110	0.4	-0.1	0.3	0.78	0.71
	June 15b	1115	0.6	-0.4	0.6	0.63	0.53
	June 18a	633	0.1	0.0	0.1	0.48	0.52
	June 19a	1071	0.4	-0.3	0.3	0.65	0.47
	June 21a	1075	0.3	-0.1	0.2	0.48	0.62
	June 21b	1126	0.3	-0.1	0.2	0.47	0.55
	June 23a	1079	0.8	-0.4	0.6	0.76	0.70
	June 23b	1106	0.9	-0.8	1.1	0.63	0.49
	June 24a	1173	0.3	-0.2	0.4	0.28	0.42
	June 24b	1034	1.0	-0.9	1.3	0.11	0.47
	June 27a	840	1.4	-0.9	1.6	0.84	0.60
	June 28a	1106	2.3	-1.7	2.4	0.64	0.51
	June 28b	755	0.9	-0.5	0.8	0.17	0.45

Table S25. Performance of simulated toluene from the DEF_ANT simulation in terms of bias, RMSE, R, and IA for each for the G-1 flights.

Variable	Flight Date	Number of Data Points	Observed Mean	Bias	RMSE	R	IA
	June 03a	851	0.1	-0.1	0.2	0.32	0.51
	June 06a	—	—	—	—	—	—
	June 06b	705	0.1	0.0	0.0	0.26	0.54
	June 08a	1190	0.1	0.0	0.1	0.40	0.52
	June 08b	1140	0.0	0.1	0.1	0.45	0.45
	June 10a	1113	0.0	0.0	0.0	0.03	0.39
	June 12a	1114	0.0	0.0	0.0	0.23	0.51
	June 12b	—	—	—	—	—	—
	June 14a	1168	0.1	0.1	0.2	0.25	0.48
	June 15a	1110	0.1	0.2	0.2	0.43	0.31
toluene (ppbv)	June 15b	1115	0.1	0.0	0.1	0.23	0.49
	June 18a	633	0.1	0.0	0.1	0.21	0.53
	June 19a	1071	0.1	0.0	0.0	0.40	0.64
	June 21a	1075	0.1	0.1	0.1	0.43	0.56
	June 21b	1126	0.1	0.0	0.1	0.11	0.40
	June 23a	1079	0.1	0.0	0.2	0.45	0.49
	June 23b	1106	0.1	0.0	0.1	-0.01	0.38
	June 24a	1173	0.1	0.0	0.1	0.21	0.40
	June 24b	1034	0.1	0.1	0.2	0.33	0.45
	June 27a	840	0.1	0.0	0.1	0.58	0.63
	June 28a	1106	0.2	0.2	0.3	0.49	0.49
	June 28b	755	0.1	-0.1	0.1	0.24	0.46

Table S26. Performance of simulated terpene (TERP) from the DEF_ANT simulation in terms of bias, RMSE, R, and IA for each for the G-1 flights.

Variable	Flight Date	Number of Data Points	Observed Mean	Bias	RMSE	R	IA
	June 03a	854	0.0	0.0	0.1	0.43	0.43
	June 06a	1133	0.0	0.0	0.1	0.02	0.37
	June 06b	705	0.0	0.0	0.1	0.02	0.27
	June 08a	1190	0.0	0.0	0.1	0.05	0.44
	June 08b	1140	0.0	0.0	0.1	0.07	0.40
	June 10a	1113	0.0	0.0	0.0	0.01	0.39
	June 12a	1114	0.0	0.0	0.0	0.10	0.43
	June 12b	—	—	—	—	—	—
	June 14a	1168	0.1	-0.1	0.1	-0.03	0.41
	June 15a	1110	0.0	0.0	0.1	-0.09	0.39
TERP (ppbv)	June 15b	1115	0.1	-0.1	0.1	0.28	0.46
	June 18a	633	0.1	0.0	0.1	0.16	0.45
	June 19a	1071	0.1	-0.1	0.1	-0.08	0.42
	June 21a	1075	0.1	0.0	0.1	0.14	0.45
	June 21b	1126	0.1	-0.1	0.1	0.15	0.44
	June 23a	1079	0.1	-0.1	0.1	0.35	0.50
	June 23b	1106	0.1	-0.1	0.1	0.23	0.43
	June 24a	1173	0.1	-0.1	0.1	0.07	0.44
	June 24b	1034	0.1	-0.1	0.1	-0.16	0.41
	June 27a	840	0.1	-0.1	0.1	0.46	0.51
	June 28a	1106	0.1	-0.1	0.1	0.25	0.46
	June 28b	755	0.1	-0.1	0.1	0.16	0.44

Table S27. Performance of simulated carbon monoxide (CO) from the DEF_ANT simulation in terms of bias, RMSE, R, and IA for each for the WP-3D flights.

Variable	Flight Date	Number of Data Points		Observed Mean	Bias	RMSE	R	IA
CO (ppbV)	May 4	16011	166.3	42.5	69.4	0.75	0.79	
	May 7	23212	161.7	9.3	35.5	0.78	0.86	
	May 8	24182	177.0	8.6	44.2	0.80	0.89	
	May 11	24549	145.6	0.0	13.6	0.82	0.90	
	May 12	26169	153.7	10.4	26.4	0.85	0.90	
	May 14	20857	172.1	29.6	56.4	0.83	0.87	
	May 16	26495	168.6	30.0	50.9	0.90	0.89	
	May 19	22960	173.5	15.9	52.3	0.86	0.92	
	May 212	10366	150.8	-5.7	16.6	0.90	0.94	
	May 22	21538	142.3	0.2	20.3	0.80	0.84	
	May 23	19728	150.9	27.5	59.4	0.57	0.58	
	May 24	20125	164.2	49.9	80.8	0.76	0.69	
	May 25	21126	158.6	12.9	34.4	0.73	0.83	
	June 3	22894	179.3	27.0	61.2	0.80	0.86	
	June 14	25077	123.3	11.0	30.2	0.82	0.89	
	June 16	23692	133.2	8.1	35.4	0.82	0.80	
	June 18	24262	120.2	6.9	20.3	0.88	0.92	
	June 20	24350	164.8	21.0	54.2	0.79	0.79	
	June 22	4536	136.3	25.9	50.9	0.62	0.68	

Table S28. Performance of simulated nitrogen oxide (NO) from the DEF_ANT simulation in terms of bias, RMSE, R, and IA for each for the WP-3D flights.

Variable	Number						
	Flight Date	of Data Points	Observed Mean	Bias	RMSE	R	IA
NO (ppbV)	May 4	15868	1.0	0.6	2.4	0.63	0.74
	May 7	23049	0.4	0.4	1.5	0.59	0.72
	May 8	23923	0.6	0.2	2.7	0.19	0.32
	May 11	21719	0.4	0.1	0.7	0.87	0.91
	May 12	25402	0.6	0.1	1.5	0.65	0.78
	May 14	—	—	—	—	—	—
	May 16	26574	0.2	0.5	1.5	0.72	0.56
	May 19	22654	2.3	1.0	3.5	0.77	0.83
	May 21	8785	0.8	-0.3	3.0	0.49	0.54
	May 22	20434	0.1	0.2	1.3	0.60	0.54
	May 23	19471	0.0	0.0	0.9	0.46	0.14
	May 24	19906	0.0	0.1	1.2	0.28	0.28
	May 25	21034	0.1	0.2	2.1	0.17	0.07
	June 3	22893	0.2	0.3	1.8	0.62	0.71
	June 14	23681	0.2	0.1	1.4	0.80	0.84
	June 16	23026	0.4	0.3	1.7	0.87	0.76
	June 18	23687	0.3	0.2	1.0	0.77	0.74
	June 20	23911	0.4	1.7	5.1	0.37	0.19
	June 22	4357	0.4	0.1	1.6	0.50	0.67

Table S29. Performance of simulated nitrogen dioxide (NO_2) from the DEF_ANT simulation in terms of bias, RMSE, R, and IA for each for the WP-3D flights.

Variable	Flight Date	Number of Data Points	Observed			
			Mean	Bias	RMSE	R
NO_2 (ppbV)	May 4	13716	3.0	1.1	4.7	0.73
	May 7	19543	1.3	1.1	4.7	0.35
	May 8	23562	2.0	0.4	3.3	0.63
	May 11	20335	0.9	0.1	0.9	0.91
	May 12	24752	1.6	0.2	2.4	0.82
	May 14	—	—	—	—	—
	May 16	25836	0.9	1.5	3.9	0.87
	May 19	22016	4.1	1.2	4.1	0.85
	May 212	8569	1.1	-0.1	2.4	0.69
	May 22	19838	0.9	0.7	1.9	0.85
	May 23	19019	1.4	2.6	5.7	0.61
	May 24	19676	1.5	3.5	7.1	0.61
	May 25	20812	1.5	0.9	4.1	0.54
	June 3	22697	2.3	4.1	8.3	0.52
	June 14	22767	0.8	0.4	2.1	0.83
	June 16	22390	1.0	0.6	2.3	0.91
	June 18	23234	0.9	0.4	1.5	0.84
	June 20	23475	1.1	2.6	6.0	0.61
	June 22	4228	0.9	0.3	2.5	0.52
						0.69

Table S30. Performance of simulated ammonia (NH_3) from the DEF_ANT simulation in terms of bias, RMSE, R, and IA for each for the WP-3D flights.

Variable	Flight Date	Number of Data Points	Observed			
			Mean	Bias	RMSE	R
NH_3 (ppbV)	May 4	8506	3.7	-1.6	8.9	0.44
	May 7	14716	24.2	-19.5	42.9	0.56
	May 8	13058	5.0	-2.9	7.7	0.59
	May 11	10948	4.3	-3.3	4.7	0.49
	May 12	16250	11.2	-8.7	17.9	0.70
	May 14	14387	5.3	-3.5	12.2	0.57
	May 16	20454	3.2	-1.8	13.1	0.42
	May 19	18686	13.3	-10.9	49.3	0.54
	May 21	8783	1.7	-0.9	5.0	0.47
	May 22	17075	5.8	-3.3	15.6	0.17
	May 23	18552	0.9	0.5	2.1	0.46
	May 24	18966	3.0	-0.9	9.2	0.18
	May 25	19875	3.3	-1.4	11.3	0.46
	June 3	17383	3.2	-0.9	6.9	0.03
	June 14	19974	4.1	-2.8	5.7	0.75
	June 16	21467	7.8	-4.2	10.4	0.65
	June 18	19080	7.7	-5.9	18.0	0.35
	June 20	22002	2.4	-0.2	4.0	0.47
	June 22	3573	5.7	-3.9	8.0	0.68

Table S31. Performance of simulated sulfur dioxide (SO_2) from the DEF_ANT simulation in terms of bias, RMSE, R, and IA for each for the WP-3D flights.

Variable	Number						
	Flight Date	of Data Points	Observed Mean	Bias	RMSE	R	IA
SO_2 (ppbV)	May 4	15413	0.4	-0.1	0.8	0.41	0.60
	May 7	22412	0.8	-0.5	0.9	0.38	0.54
	May 8	23025	0.7	-0.3	0.9	0.45	0.62
	May 11	23401	0.1	0.0	0.3	0.44	0.61
	May 12	24820	0.4	-0.3	0.7	0.31	0.49
	May 14	20161	0.5	0.0	0.6	0.80	0.89
	May 16	25416	0.3	0.1	0.7	0.40	0.53
	May 19	22073	0.3	0.0	0.6	0.58	0.74
	May 212	9942	0.3	-0.3	1.2	0.15	0.16
	May 22	20576	0.4	-0.3	0.6	0.26	0.50
	May 23	19016	0.4	-0.1	1.4	0.24	0.23
	May 24	19306	0.6	-0.1	1.1	0.44	0.52
	May 25	20316	0.4	-0.1	1.1	0.16	0.24
	June 3	22020	0.6	-0.1	0.7	0.47	0.62
	June 14	23709	0.4	-0.2	0.6	0.49	0.53
	June 16	22677	0.7	-0.5	0.9	0.22	0.47
	June 18	23319	0.4	-0.2	0.7	0.27	0.49
	June 20	23384	0.4	0.3	1.6	0.26	0.29
	June 22	4307	0.5	-0.2	0.9	0.11	0.35

Table S32. Performance of simulated ozone (O_3) from the DEF_ANT simulation in terms of bias, RMSE, R, and IA for each for the WP-3D flights.

Variable	Flight Date	Number of Data Points	Observed				
			Mean	Bias	RMSE	R	IA
O_3 (ppbV)	May 4	16552	68.0	-2.3	8.5	0.54	0.71
	May 7	23787	62.6	-5.4	10.0	0.60	0.70
	May 8	24401	75.7	-8.9	12.4	0.75	0.75
	May 11	25079	50.9	-4.1	15.9	0.69	0.69
	May 12	26879	51.7	4.0	10.6	0.52	0.64
	May 14	—	—	—	—	—	—
	May 16	27326	66.6	-1.5	13.1	0.63	0.78
	May 19	23389	51.3	-4.8	11.1	0.58	0.71
	May 21	9855	57.5	-10.4	13.4	0.87	0.74
	May 22	21551	56.7	-12.6	14.8	0.69	0.55
	May 23	20158	63.9	-10.8	13.5	0.61	0.59
	May 24	20628	63.4	-9.0	14.2	0.39	0.52
	May 25	21733	49.9	-2.2	13.5	0.43	0.65
	June 3	23712	53.3	-14.9	21.2	0.19	0.46
	June 14	24837	58.8	1.7	9.7	0.74	0.86
	June 16	24068	55.0	-4.6	9.1	0.77	0.84
	June 18	24639	51.2	-4.8	10.2	0.79	0.85
	June 20	24574	66.9	-10.7	16.0	0.51	0.64
	June 22	4598	68.7	-5.1	12.1	0.44	0.59

Table S33. Performance of simulated isoprene from the DEF_ANT simulation in terms of bias, RMSE, R, and IA for each for the WP-3D flights.

Variable	Flight Date	Number of Data Points	Observed				IA
			Mean	Bias	RMSE	R	
isoprene (ppbV)	May 4	616	0.1	0.0	0.1	0.53	0.71
	May 7	937	0.1	0.0	0.1	0.63	0.77
	May 8	1371	0.1	0.0	0.1	0.56	0.73
	May 11	1118	0.0	0.0	0.0	0.52	0.70
	May 12	1464	0.0	0.0	0.1	0.68	0.81
	May 14	1160	0.1	0.0	0.1	0.84	0.88
	May 16	1448	0.0	0.0	0.1	0.75	0.81
	May 19	912	0.1	0.0	0.1	0.76	0.85
	May 21	465	0.0	0.0	0.0	0.69	0.78
	May 22	1222	0.0	0.0	0.0	0.56	0.67
	May 23	1122	0.0	0.0	0.1	0.36	0.56
	May 24	1149	0.0	0.0	0.1	0.15	0.38
	May 25	1199	0.0	0.0	0.0	0.18	0.37
	June 3	1300	0.0	0.0	0.0	0.18	0.42
	June 14	1326	0.1	0.0	0.2	0.66	0.78
	June 16	1077	0.0	0.0	0.1	0.52	0.70
	June 18	808	0.0	0.0	0.1	0.47	0.68
	June 20	1419	0.1	0.0	0.1	0.59	0.74
	June 22	267	0.1	0.0	0.2	0.35	0.52

Table S34. Performance of simulated methyl-vinyl-ketone + methacrolein (MVK+MACR) from the DEF_ANT simulation in terms of bias, RMSE, R, and IA for each for the WP-3D flights.

Variable	Flight Date	Number of Data Points	Observed Mean	Bias	RMSE	R	IA
MVK+ MACR (ppbV)	May 4	70	0.2	0.0	0.2	0.00	0.16
	May 7	70	0.1	0.1	0.1	0.08	0.42
	May 8	71	0.2	0.1	0.1	0.21	0.49
	May 11	71	0.1	0.0	0.1	-0.19	0.28
	May 12	70	0.1	0.1	0.1	-0.33	0.30
	May 14	70	0.1	0.0	0.1	-0.48	0.12
	May 16	71	0.1	0.1	0.1	0.08	0.37
	May 19	71	0.1	0.1	0.1	-0.02	0.39
	May 212	71	-0.1	0.2	0.5	0.23	0.28
	May 22	71	-0.3	0.4	0.7	0.55	0.39
	May 23	58	-0.1	0.3	0.6	0.21	0.38
	May 24	71	-0.1	0.2	0.5	-0.12	0.27
	May 25	65	-0.1	0.2	0.5	0.09	0.30
	June 3	71	0.0	0.1	0.5	0.07	0.20
	June 14	71	-0.1	0.3	0.8	-0.23	0.33
	June 16	70	-0.2	0.4	0.7	-0.25	0.37
	June 18	71	-0.1	0.4	0.7	0.08	0.36
	June 20	71	-0.2	0.5	0.9	0.10	0.41
	June 22	71	0.2	0.0	0.3	-0.16	0.12

Table S35. Performance of simulated terpene (TERP) from the DEF_ANT simulation in terms of bias, RMSE, R, and IA for each for the WP-3D flights.

Variable	Flight Date	Number of Data Points	Observed				
			Mean	Bias	RMSE	R	IA
TERP (ppbv)	May 4	745	0.0	0.0	0.0	0.51	0.46
	May 7	1147	0.0	0.0	0.0	0.28	0.41
	May 8	1202	0.0	0.0	0.0	0.50	0.49
	May 11	1282	0.0	0.0	0.0	0.18	0.38
	May 12	1464	0.0	0.0	0.0	0.46	0.41
	May 14	1160	0.0	0.0	0.0	0.75	0.65
	May 16	1448	0.0	0.0	0.0	0.54	0.59
	May 19	1247	0.0	0.0	0.1	0.60	0.50
	May 21	573	0.0	0.0	0.0	0.77	0.25
	May 22	1221	0.0	0.0	0.0	0.24	0.21
	May 23	1122	0.0	0.0	0.0	0.44	0.56
	May 24	1148	0.0	0.0	0.0	0.42	0.49
	May 25	1198	0.0	0.0	0.0	0.13	0.24
	June 3	1300	0.0	0.0	0.0	0.18	0.40
	June 14	1326	0.0	0.0	0.0	0.25	0.32
	June 16	1388	0.0	0.0	0.0	0.49	0.32
	June 18	1177	0.0	0.0	0.0	0.27	0.19
	June 20	1302	0.0	0.0	0.0	0.42	0.59
	June 22	266	0.0	0.0	0.1	0.65	0.28

Table S36. Performance of simulated formaldehyde (CH_2O) from the DEF_ANT simulation in terms of bias, RMSE, R, and IA for each for the WP-3D flights.

Variable	Flight Date	Number of Data Points		Observed Mean		RMSE	R	IA
				Bias				
CH_2O (ppbv)	May 4	780	1.9	-0.4	0.9	0.81	0.86	
	May 7	1323	1.7	-0.4	0.7	0.75	0.79	
	May 8	1372	2.1	-1.0	1.3	0.83	0.73	
	May 11	1379	0.9	-0.3	0.5	0.56	0.64	
	May 12	1464	1.4	-0.4	0.6	0.76	0.79	
	May 14	1200	1.6	-0.4	0.9	0.78	0.83	
	May 16	1501	1.6	-0.5	0.9	0.88	0.86	
	May 19	1306	2.1	-0.8	1.2	0.85	0.79	
	May 212	574	1.1	-0.5	0.7	0.73	0.69	
	May 22	1222	1.1	-0.3	0.5	0.50	0.58	
	May 23	1123	1.8	-0.3	0.7	0.72	0.79	
	May 24	1150	2.1	-0.3	0.8	0.73	0.79	
	May 25	1199	2.0	-0.8	1.0	0.55	0.56	
	June 3	1300	2.6	-1.0	1.2	0.80	0.66	
	June 14	1478	2.9	-1.3	1.6	0.84	0.77	
	June 16	1388	2.1	-0.8	1.0	0.72	0.66	
	June 18	1388	2.1	-0.9	1.3	0.31	0.50	
	June 20	1419	2.7	-1.3	1.5	0.81	0.66	
	June 22	267	2.7	-1.5	1.6	0.50	0.44	

Table S37. Performance of simulated black carbon (BC) from the DEF_ANT simulation in terms of bias, RMSE, R, and IA for each for the G-1, WP-3D, and CIRPAS Twin Otter flights.

Flight Date	Number of Data Points	Observed Mean ($\mu\text{g}/\text{m}^3$)	Bias ($\mu\text{g}/\text{m}^3$)	RMSE	R	IA
G-1, June 03a	787	0.03	0.03	0.04	0.36	0.40
G-1, June 06a	1083	0.02	0.08	0.09	0.54	0.24
G-1, June 06b	658	0.02	0.07	0.09	0.10	0.14
G-1, June 08a	1144	0.09	0.07	0.10	0.10	0.36
G-1, June 08b	883	0.07	0.08	0.09	0.67	0.41
G-1, June 10a	786	0.03	0.03	0.04	0.32	0.29
G-1, June 12a	1090	0.02	0.05	0.06	0.47	0.24
G-1, June 12b	713	0.02	0.05	0.05	-0.02	0.16
G-1, June 14a	1139	0.08	0.10	0.12	0.50	0.48
G-1, June 15a	1075	0.07	0.16	0.16	0.65	0.32
G-1, June 15b	830	0.09	0.08	0.09	0.58	0.46
G-1, June 18a	786	0.05	0.04	0.07	0.17	0.33
G-1, June 19a	—	—	—	—	—	—
G-1, June 21a	1107	0.07	0.12	0.18	0.21	0.31
G-1, June 21b	797	0.06	0.05	0.08	0.42	0.53
G-1, June 23a	1145	0.09	0.09	0.10	0.44	0.39
G-1, June 23b	769	0.10	0.09	0.10	0.36	0.40
G-1, June 24a	1140	0.06	0.07	0.10	0.06	0.36
G-1, June 24b	703	0.08	0.05	0.08	0.48	0.61
G-1, June 27a	1185	0.07	0.15	0.16	0.73	0.27
G-1, June 28a	1091	0.13	0.17	0.21	0.56	0.51
G-1, June 28b	579	0.11	0.06	0.09	0.11	0.42
WP-3D, May 4	8197	0.02	0.13	0.14	0.59	0.27
WP-3D, May 7	24831	0.08	0.07	0.12	0.73	0.74
WP-3D, May 8	25375	0.09	0.09	0.15	0.66	0.63
WP-3D, May 11	25780	0.03	0.05	0.08	0.65	0.64
WP-3D, May 12	25020	0.08	0.06	0.10	0.68	0.73
WP-3D, May 14	19087	0.14	0.12	0.19	0.79	0.80
WP-3D, May 16	21321	0.09	0.16	0.22	0.75	0.53
WP-3D, May 19	24221	0.15	0.06	0.15	0.80	0.87
WP-3D, May 21	10357	0.05	0.02	0.05	0.88	0.92
WP-3D, May 22	22536	0.03	0.05	0.08	0.55	0.60
WP-3D, May 23	20827	0.04	0.11	0.16	0.63	0.45
WP-3D, May 24	20661	0.07	0.14	0.22	0.44	0.46
WP-3D, May 25	20469	0.09	0.08	0.17	0.49	0.54
WP-3D, June 3	23570	0.16	0.07	0.15	0.66	0.77
WP-3D, June 14	26406	0.07	0.05	0.16	0.51	0.62

WP-3D, June 16	22634	0.07	0.04	0.08	0.75	0.78
WP-3D, June 18	24707	0.05	0.04	0.07	0.77	0.83
WP-3D, June 20	24681	0.07	0.14	0.23	0.67	0.46
WP-3D, June 22	4907	0.07	0.08	0.15	0.67	0.72
Twin Otter, May 6	179	0.16	0.34	0.37	0.51	0.27
Twin Otter, May 7	194	0.22	0.36	0.51	0.61	0.30
Twin Otter, May 10	186	0.07	0.19	0.21	0.51	0.22
Twin Otter, May 12	195	0.14	0.24	0.32	0.63	0.37
Twin Otter, May 13	178	0.12	0.31	0.48	0.26	0.19
Twin Otter, May 14	189	0.15	0.44	0.48	0.42	0.23
Twin Otter, May 15	185	0.16	0.34	0.39	0.35	0.22
Twin Otter, May 18	183	0.03	0.07	0.09	0.62	0.41
Twin Otter, May 19	116	0.18	0.39	0.43	0.25	0.25
Twin Otter, May 20	192	0.06	0.08	0.12	0.92	0.69
Twin Otter, May 21	192	0.15	0.20	0.25	0.33	0.33
Twin Otter, May 22	195	0.03	0.04	0.07	0.76	0.47
Twin Otter, May 24	173	0.07	0.08	0.09	0.89	0.68
Twin Otter, May 25	191	0.10	0.12	0.14	0.80	0.53
Twin Otter, May 27	176	0.11	0.20	0.23	0.08	0.21
Twin Otter, May 28	192	0.16	0.20	0.37	-0.12	0.13

Table S38. Performance of simulated organic aerosol (OA) from the DEF_ANT simulation in terms of bias, RMSE, R, and IA for each for the G-1, WP-3D, and CIRPAS Twin Otter flights.

Flight Date	Number of Data Points	Observed Mean ($\mu\text{g}/\text{m}^3$)	Bias ($\mu\text{g}/\text{m}^3$)	RMSE	R	IA
G-1, June 03a	674	0.88	-0.09	0.67	0.37	0.64
G-1, June 06a	918	1.90	-0.78	1.25	0.53	0.59
G-1, June 06b	510	2.05	-0.94	1.66	0.13	0.48
G-1, June 08a	946	4.02	-1.67	2.30	0.76	0.65
G-1, June 08b	957	3.92	-1.26	1.67	0.79	0.78
G-1, June 10a	882	1.17	-0.35	0.52	0.49	0.58
G-1, June 12a	882	0.91	-0.51	0.61	0.47	0.47
G-1, June 12b	793	2.17	-1.54	1.66	-0.33	0.29
G-1, June 14a	928	4.08	-2.32	2.65	0.52	0.47
G-1, June 15a	878	2.64	-0.45	1.31	0.25	0.50
G-1, June 15b	882	4.93	-0.97	1.99	0.46	0.60
G-1, June 18a	922	2.14	-0.36	2.13	0.12	0.35
G-1, June 19a	887	2.16	0.30	1.00	0.45	0.66
G-1, June 21a	898	3.05	-1.55	2.48	0.45	0.49
G-1, June 21b	894	3.23	-1.38	1.90	0.59	0.59
G-1, June 23a	942	6.12	-1.99	3.01	0.48	0.57
G-1, June 23b	874	6.25	-0.81	2.17	0.53	0.64
G-1, June 24a	934	2.07	-0.22	1.84	0.13	0.45
G-1, June 24b	816	3.21	-1.33	2.28	0.28	0.51
G-1, June 27a	960	9.73	-4.88	5.68	0.69	0.59
G-1, June 28a	902	13.42	-7.60	8.87	0.75	0.54
G-1, June 28b	668	10.83	-7.02	8.45	0.60	0.47
WP-3D, May 4	1495	1.51	1.30	1.75	0.79	0.77
WP-3D, May 7	2383	2.02	0.36	1.03	0.84	0.90
WP-3D, May 8	2304	2.03	0.01	1.18	0.81	0.89
WP-3D, May 11	244	0.12	0.29	0.43	0.70	0.73
WP-3D, May 12	—	—	—	—	—	—
WP-3D, May 14	1765	1.92	1.18	1.91	0.70	0.76
WP-3D, May 16	2012	2.29	0.66	2.02	0.66	0.79
WP-3D, May 19	2102	1.85	0.20	1.21	0.87	0.91
WP-3D, May 21	434	1.14	-0.37	1.23	0.79	0.78
WP-3D, May 22	1912	0.67	0.44	0.73	0.54	0.67
WP-3D, May 23	1906	1.04	0.30	0.71	0.66	0.75
WP-3D, May 24	1938	1.86	0.00	1.30	0.71	0.77
WP-3D, May 25	1879	1.52	0.39	0.97	0.48	0.67
WP-3D, June 3	2215	2.37	0.08	1.19	0.70	0.83
WP-3D, June 14	2438	1.88	-0.22	1.62	0.74	0.83

WP-3D, June 16	2367	1.65	0.17	0.87	0.80	0.89
WP-3D, June 18	2341	1.00	0.31	0.88	0.75	0.84
WP-3D, June 20	2389	2.66	-0.97	2.00	0.83	0.73
WP-3D, June 22	481	1.01	0.94	1.51	0.29	0.51
Twin Otter, May 18	183	1.80	-0.58	1.31	0.69	0.74
Twin Otter, May 19	146	3.51	0.77	1.16	0.51	0.62
Twin Otter, May 20	192	1.30	0.40	0.71	0.92	0.94
Twin Otter, May 21	192	2.27	0.55	0.88	0.68	0.74
Twin Otter, May 22	195	0.93	-0.19	0.44	0.86	0.90
Twin Otter, May 24	173	1.50	0.17	0.67	0.64	0.78
Twin Otter, May 25	191	1.10	1.32	1.54	0.45	0.43
Twin Otter, May 27	176	2.00	-0.39	0.76	0.15	0.47
Twin Otter, May 28	192	2.27	-0.09	0.96	0.05	0.43

Table S39. Performance of simulated sulfate (SO_4^{2-}) from the DEF_ANT simulation in terms of bias, RMSE, R, and IA for each for the G-1, WP-3D, and CIRPAS Twin Otter flights.

Flight Date	Number of Data Points	Observed Mean ($\mu\text{g}/\text{m}^3$)	Bias ($\mu\text{g}/\text{m}^3$)	RMSE	R	IA
G-1, June 03a	674	0.51	-0.04	0.24	-0.16	0.28
G-1, June 06a	918	0.32	0.06	0.23	0.16	0.35
G-1, June 06b	510	0.44	-0.12	0.18	-0.23	0.35
G-1, June 08a	946	0.72	-0.24	0.34	0.16	0.45
G-1, June 08b	957	0.88	-0.20	0.37	0.59	0.70
G-1, June 10a	882	0.25	0.06	0.13	0.30	0.52
G-1, June 12a	882	0.13	0.17	0.18	-0.11	0.30
G-1, June 12b	793	0.12	0.16	0.17	-0.05	0.31
G-1, June 14a	928	0.40	0.18	0.30	0.57	0.69
G-1, June 15a	878	0.54	-0.08	0.17	0.56	0.60
G-1, June 15b	882	0.67	-0.07	0.22	0.39	0.60
G-1, June 18a	926	0.28	0.05	0.23	0.18	0.47
G-1, June 19a	887	0.46	0.45	0.56	0.23	0.30
G-1, June 21a	899	0.39	0.04	0.19	-0.03	0.36
G-1, June 21b	894	0.39	0.04	0.19	0.39	0.60
G-1, June 23a	944	0.58	-0.13	0.29	0.19	0.47
G-1, June 23b	874	0.91	-0.31	0.44	0.43	0.51
G-1, June 24a	934	0.69	-0.15	0.41	0.30	0.56
G-1, June 24b	816	0.65	-0.06	0.39	0.30	0.59
G-1, June 27a	960	0.75	-0.04	0.32	0.63	0.71
G-1, June 28a	902	0.72	-0.13	0.39	0.17	0.42
G-1, June 28b	668	0.79	-0.34	0.52	0.41	0.48
WP-3D, May 4	1495	0.42	0.17	0.29	0.70	0.76
WP-3D, May 7	2383	0.49	-0.09	0.31	0.42	0.60
WP-3D, May 8	2304	0.78	-0.18	0.76	0.18	0.38
WP-3D, May 11	244	0.32	-0.03	0.22	0.36	0.61
WP-3D, May 12	—	—	—	—	—	—
WP-3D, May 14	1765	0.93	-0.24	0.49	0.82	0.81
WP-3D, May 16	2012	1.19	-0.20	0.53	0.73	0.82
WP-3D, May 19	2105	0.75	-0.19	0.37	0.83	0.81
WP-3D, May 21	434	0.74	-0.37	0.42	0.61	0.47
WP-3D, May 22	1912	0.51	-0.24	0.32	0.20	0.44
WP-3D, May 23	1907	0.35	0.12	0.27	0.41	0.59
WP-3D, May 24	1938	0.59	0.05	0.28	0.83	0.90
WP-3D, May 25	1879	1.16	-0.39	0.59	0.70	0.73
WP-3D, June 3	2215	1.26	-0.44	0.72	0.51	0.63
WP-3D, June 14	2440	0.55	-0.16	0.34	0.56	0.64

WP-3D, June 16	2368	0.78	-0.41	0.51	0.67	0.59
WP-3D, June 18	2341	0.48	-0.14	0.28	0.64	0.69
WP-3D, June 20	2389	0.99	-0.41	0.56	0.62	0.66
WP-3D, June 22	481	0.81	-0.38	0.56	0.35	0.49
Twin Otter, May 18	183	1.13	-0.70	1.23	-0.80	0.38
Twin Otter, May 19	146	0.77	0.44	0.57	0.56	0.58
Twin Otter, May 20	192	0.57	-0.08	0.46	-0.06	0.31
Twin Otter, May 21	192	0.50	0.13	0.25	0.41	0.57
Twin Otter, May 22	195	0.47	-0.21	0.29	0.67	0.59
Twin Otter, May 24	173	0.32	-0.02	0.11	0.62	0.65
Twin Otter, May 25	191	0.17	0.32	0.33	0.56	0.25
Twin Otter, May 27	176	0.80	-0.13	0.38	0.17	0.42
Twin Otter, May 28	192	0.69	-0.10	0.41	0.38	0.41

Table S40. Performance of simulated nitrate (NO_3^-) from the DEF_ANT simulation in terms of bias, RMSE, R, and IA for each for the G-1, WP-3D, and CIRPAS Twin Otter flights.

Flight Date	Number of Data Points	Observed Mean ($\mu\text{g}/\text{m}^3$)	Bias ($\mu\text{g}/\text{m}^3$)	RMSE	R	IA
G-1, June 03a	674	0.12	0.00	0.11	0.07	0.37
G-1, June 06a	918	0.09	0.01	0.06	0.33	0.56
G-1, June 06b	510	0.10	-0.01	0.06	0.01	0.37
G-1, June 08a	946	0.21	-0.05	0.10	-0.04	0.38
G-1, June 08b	957	0.21	0.02	0.10	0.59	0.73
G-1, June 10a	882	0.07	0.02	0.05	0.07	0.39
G-1, June 12a	882	0.05	0.06	0.07	-0.08	0.40
G-1, June 12b	793	0.06	0.04	0.06	-0.05	0.43
G-1, June 14a	928	0.14	0.03	0.08	0.48	0.66
G-1, June 15a	878	0.17	-0.02	0.10	0.29	0.55
G-1, June 15b	882	0.20	0.07	0.17	0.14	0.30
G-1, June 18a	926	0.18	-0.04	0.19	0.37	0.60
G-1, June 19a	887	0.17	0.14	0.19	0.41	0.43
G-1, June 21a	899	0.14	0.01	0.08	0.12	0.41
G-1, June 21b	894	0.12	0.02	0.07	0.45	0.62
G-1, June 23a	944	0.21	-0.04	0.11	0.04	0.40
G-1, June 23b	874	0.25	-0.01	0.13	0.10	0.39
G-1, June 24a	934	0.15	0.02	0.12	0.16	0.48
G-1, June 24b	816	0.14	0.04	0.14	0.28	0.53
G-1, June 27a	960	0.21	0.02	0.08	0.62	0.75
G-1, June 28a	902	0.24	-0.04	0.10	0.44	0.55
G-1, June 28b	668	0.19	-0.03	0.10	0.50	0.52
WP-3D, May 4	1495	0.61	0.47	2.05	0.57	0.63
WP-3D, May 7	2383	0.89	0.41	1.52	0.63	0.72
WP-3D, May 8	2304	0.65	0.22	1.60	0.63	0.68
WP-3D, May 11	244	0.11	0.09	0.28	0.84	0.86
WP-3D, May 12	—	—	—	—	—	—
WP-3D, May 14	1765	0.82	0.75	2.23	0.34	0.50
WP-3D, May 16	2012	1.19	0.57	1.62	0.80	0.87
WP-3D, May 19	2105	2.95	-1.73	3.74	0.78	0.72
WP-3D, May 21	434	0.72	-0.26	0.83	0.89	0.93
WP-3D, May 22	1912	0.09	0.00	0.26	0.37	0.56
WP-3D, May 23	1907	0.07	-0.04	0.23	0.23	0.38
WP-3D, May 24	1938	0.29	0.50	1.79	0.64	0.49
WP-3D, May 25	1879	0.80	-0.13	1.22	0.59	0.76
WP-3D, June 3	2215	1.26	0.14	2.33	0.56	0.72
WP-3D, June 14	2440	0.13	-0.13	0.42	0.43	0.35

WP-3D, June 16	2368	0.36	-0.06	0.64	0.52	0.69
WP-3D, June 18	2341	0.30	-0.16	0.50	0.65	0.79
WP-3D, June 20	2389	0.45	-0.02	1.09	0.58	0.66
WP-3D, June 22	481	0.32	-0.11	0.94	0.95	0.85
Twin Otter, May 18	183	1.05	-0.53	1.39	0.65	0.73
Twin Otter, May 19	146	5.43	-2.42	3.44	0.59	0.62
Twin Otter, May 20	192	1.51	-0.20	1.99	0.49	0.67
Twin Otter, May 21	192	2.32	-1.17	2.33	0.31	0.56
Twin Otter, May 22	195	0.65	0.41	1.01	0.64	0.65
Twin Otter, May 24	173	0.94	-0.35	0.99	0.54	0.70
Twin Otter, May 25	191	0.81	0.55	1.68	0.57	0.61
Twin Otter, May 27	176	2.48	-2.22	2.89	0.32	0.47
Twin Otter, May 28	192	1.59	0.28	1.53	0.45	0.67

Table S41. Performance of simulated ammonium (NH_4^+) from the DEF_ANT simulation in terms of bias, RMSE, R, and IA for each for the G-1, WP-3D, and CIRPAS Twin Otter flights.

Flight Date	Number of Data Points	Observed Mean ($\mu\text{g}/\text{m}^3$)	Bias ($\mu\text{g}/\text{m}^3$)	RMSE	R	IA
G-1, June 03a	674	0.09	0.04	0.21	0.11	0.25
G-1, June 06a	918	0.13	-0.13	0.16	-0.22	0.43
G-1, June 06b	510	0.11	-0.11	0.14	0.01	0.42
G-1, June 08a	946	0.42	-0.35	0.41	-0.04	0.35
G-1, June 08b	957	0.29	-0.27	0.34	-0.01	0.43
G-1, June 10a	882	0.11	-0.11	0.15	0.06	0.38
G-1, June 12a	882	0.06	-0.06	0.07	-0.03	0.39
G-1, June 12b	793	0.10	-0.10	0.10	—	0.30
G-1, June 14a	928	0.34	-0.34	0.40	0.06	0.43
G-1, June 15a	878	0.47	-0.24	0.40	0.40	0.58
G-1, June 15b	882	0.53	-0.24	0.57	0.09	0.38
G-1, June 18a	926	0.60	-0.41	1.00	0.38	0.48
G-1, June 19a	887	0.25	-0.24	0.29	0.05	0.40
G-1, June 21a	899	0.31	-0.31	0.50	0.01	0.32
G-1, June 21b	894	0.19	-0.19	0.24	-0.11	0.42
G-1, June 23a	944	0.40	-0.38	0.48	-0.11	0.30
G-1, June 23b	874	0.36	-0.25	0.46	-0.02	0.30
G-1, June 24a	934	0.23	-0.20	0.31	-0.15	0.39
G-1, June 24b	816	0.25	-0.25	0.29	0.01	0.41
G-1, June 27a	960	0.43	-0.43	0.47	0.19	0.39
G-1, June 28a	902	0.61	-0.61	0.69	-0.14	0.40
G-1, June 28b	668	0.40	-0.40	0.45	-0.13	0.39
WP-3D, May 4	1495	0.36	0.12	0.67	0.57	0.70
WP-3D, May 7	2383	0.48	0.03	0.48	0.64	0.79
WP-3D, May 8	2304	0.50	-0.10	0.56	0.57	0.71
WP-3D, May 11	244	0.10	0.01	0.10	0.83	0.90
WP-3D, May 12	—	—	—	—	—	—
WP-3D, May 14	1765	0.61	0.06	0.66	0.54	0.72
WP-3D, May 16	2012	0.86	-0.01	0.55	0.82	0.90
WP-3D, May 19	2105	1.15	-0.62	1.25	0.80	0.73
WP-3D, May 21	434	0.50	-0.27	0.44	0.88	0.88
WP-3D, May 22	1912	0.20	-0.11	0.19	0.18	0.49
WP-3D, May 23	1907	0.13	0.02	0.20	0.10	0.29
WP-3D, May 24	1938	0.31	0.13	0.50	0.73	0.75
WP-3D, May 25	1879	0.64	-0.17	0.49	0.67	0.79
WP-3D, June 3	2215	0.80	-0.11	0.74	0.63	0.78
WP-3D, June 14	2440	0.18	-0.08	0.23	0.58	0.57

WP-3D, June 16	2368	0.37	-0.19	0.32	0.61	0.72
WP-3D, June 18	2341	0.21	-0.11	0.24	0.75	0.79
WP-3D, June 20	2389	0.45	-0.17	0.44	0.56	0.69
WP-3D, June 22	481	0.34	-0.14	0.42	0.90	0.77
Twin Otter, May 18	183	0.73	-0.46	0.75	0.44	0.55
Twin Otter, May 19	146	2.31	-1.01	1.33	0.47	0.53
Twin Otter, May 20	192	1.05	-0.54	0.79	0.65	0.66
Twin Otter, May 21	192	1.49	-1.03	1.28	0.30	0.49
Twin Otter, May 22	195	0.43	-0.07	0.33	0.58	0.74
Twin Otter, May 24	173	0.40	-0.16	0.39	0.49	0.65
Twin Otter, May 25	191	0.43	0.11	0.50	0.55	0.67
Twin Otter, May 27	176	1.23	-0.93	1.16	0.14	0.45
Twin Otter, May 28	192	0.85	-0.11	0.57	0.22	0.55

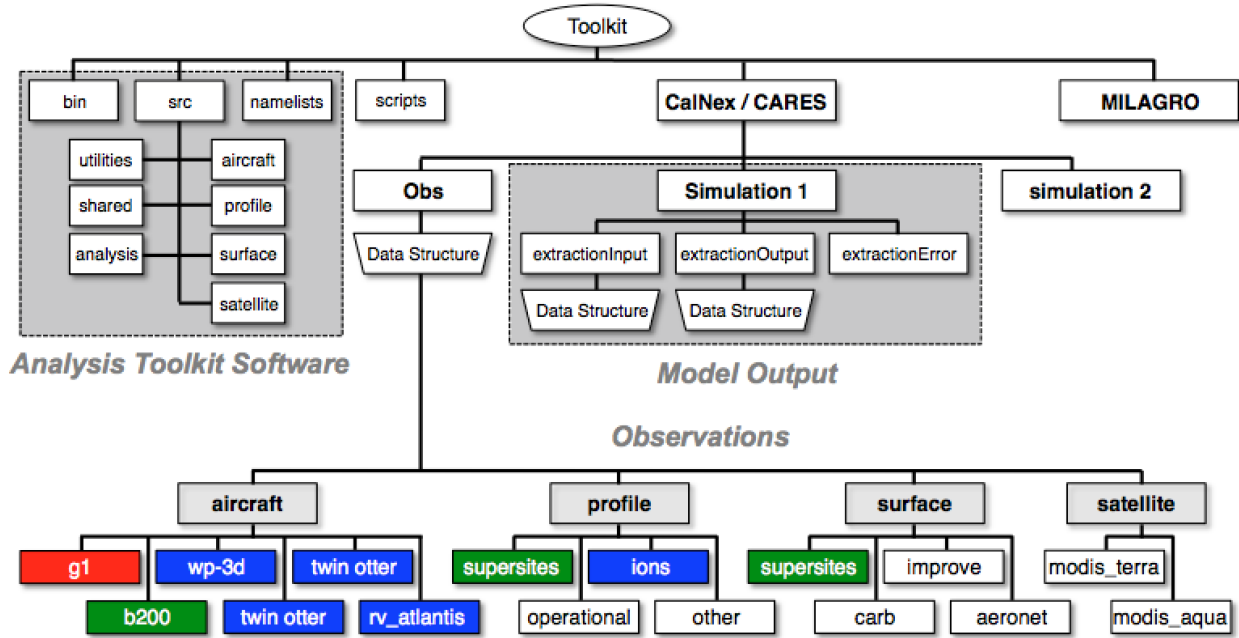


Figure S1. Directory structure of the Aerosol Modeling Testbed for the CalNex/CARES testbed case. Blue, red, and green denote data from CalNex, CARES, and both campaigns, respectively.

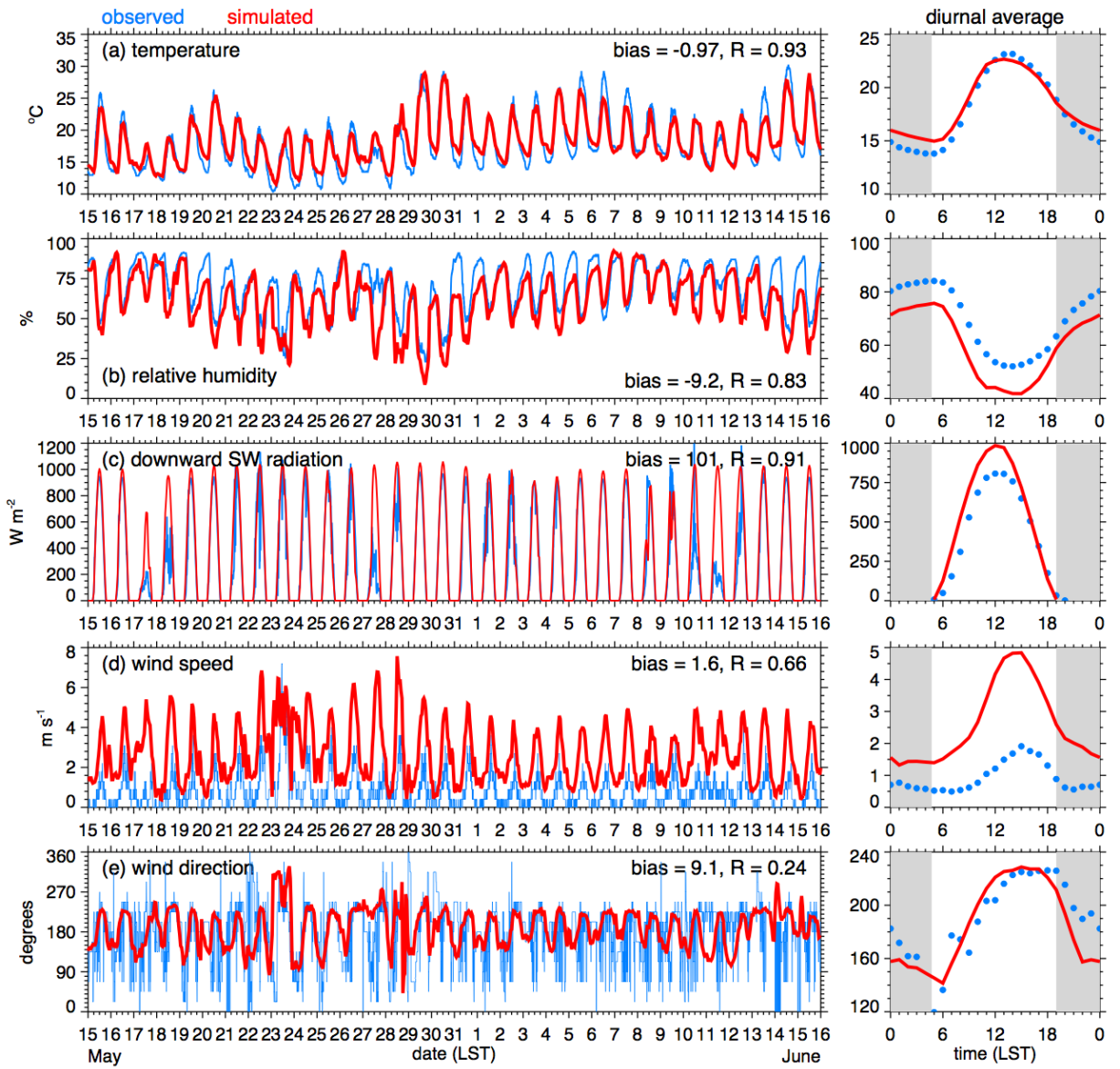


Figure S2. Time series (left panels) and diurnal average (right panels) of (a) temperature, (b) relative humidity, (c) downward shortwave radiation, (d) wind speed, and (e) wind direction at the Pasadena supersite. Observed values are hourly averages, while simulated values are instantaneous values at hourly intervals. Gray shading denotes night and R is the correlation coefficient.

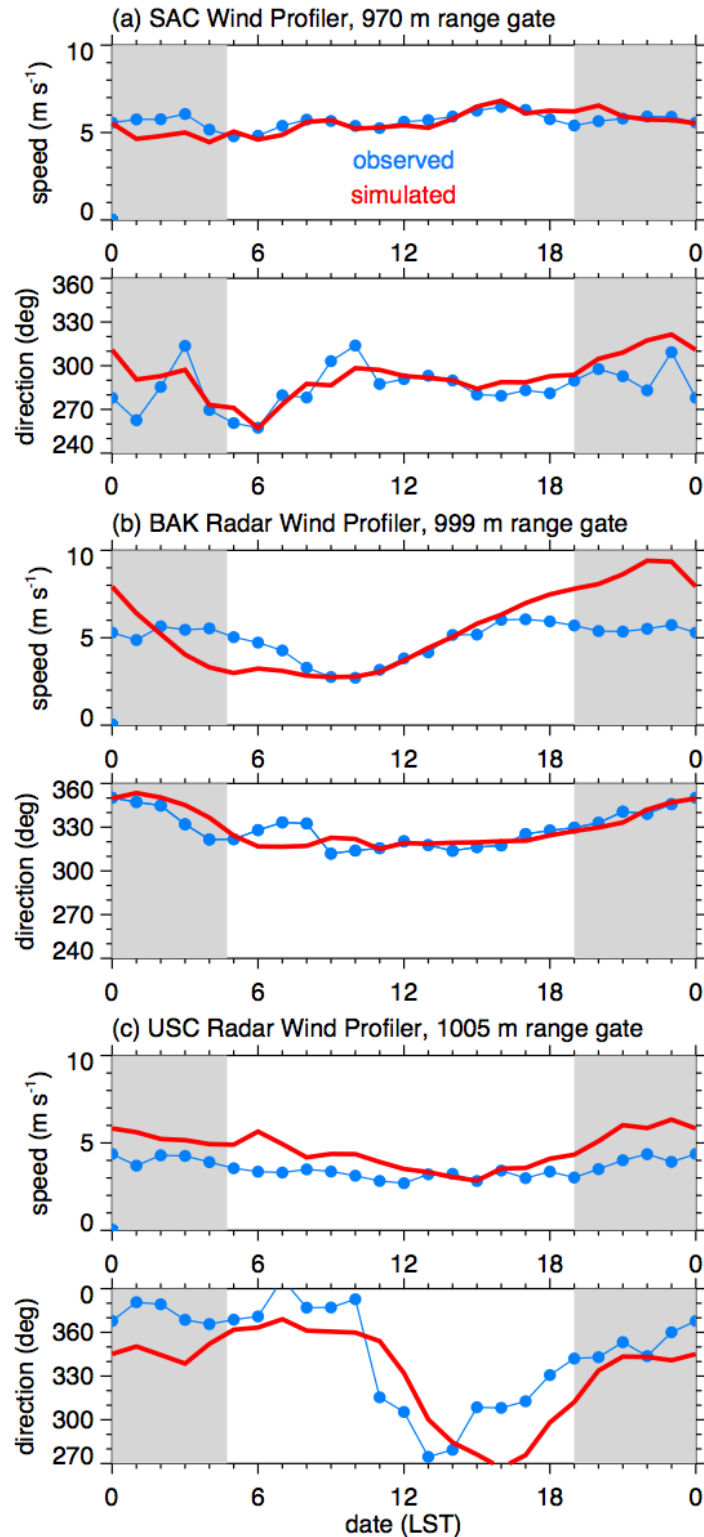


Figure S3. Observed and simulated diurnally-averaged wind speed and direction over the 2-month period approximately 1 km AGL at the (a) SAC, (b) BAK, and (c) USC radar wind profiler sites. Gray shading denotes night

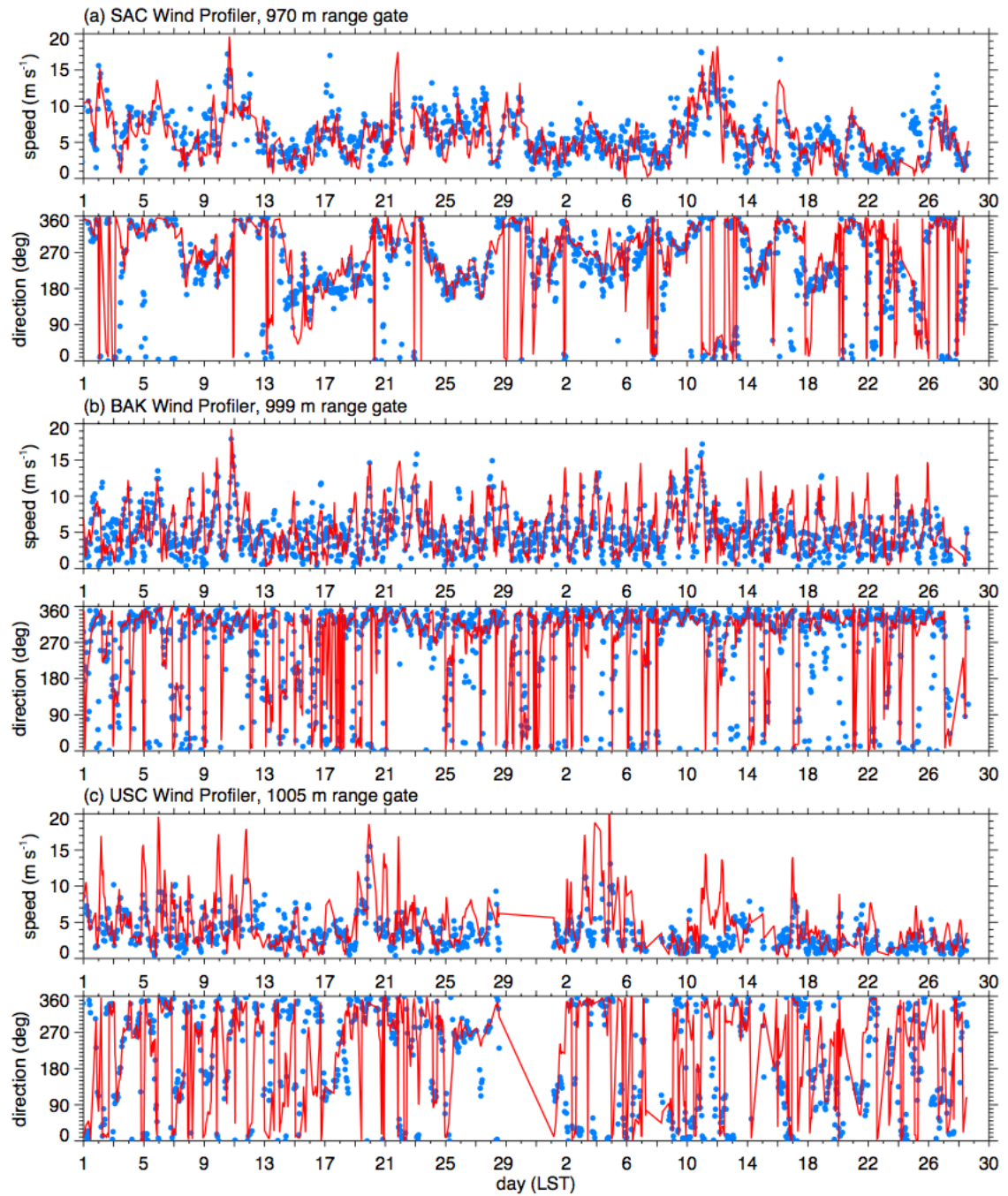


Figure S4. Comparison of observed and simulated wind speed and direction over May and June 2010 approximately 1 km AGL at the (a) SAC, (b), BAK, and (c) USC radar wind profiler sites.

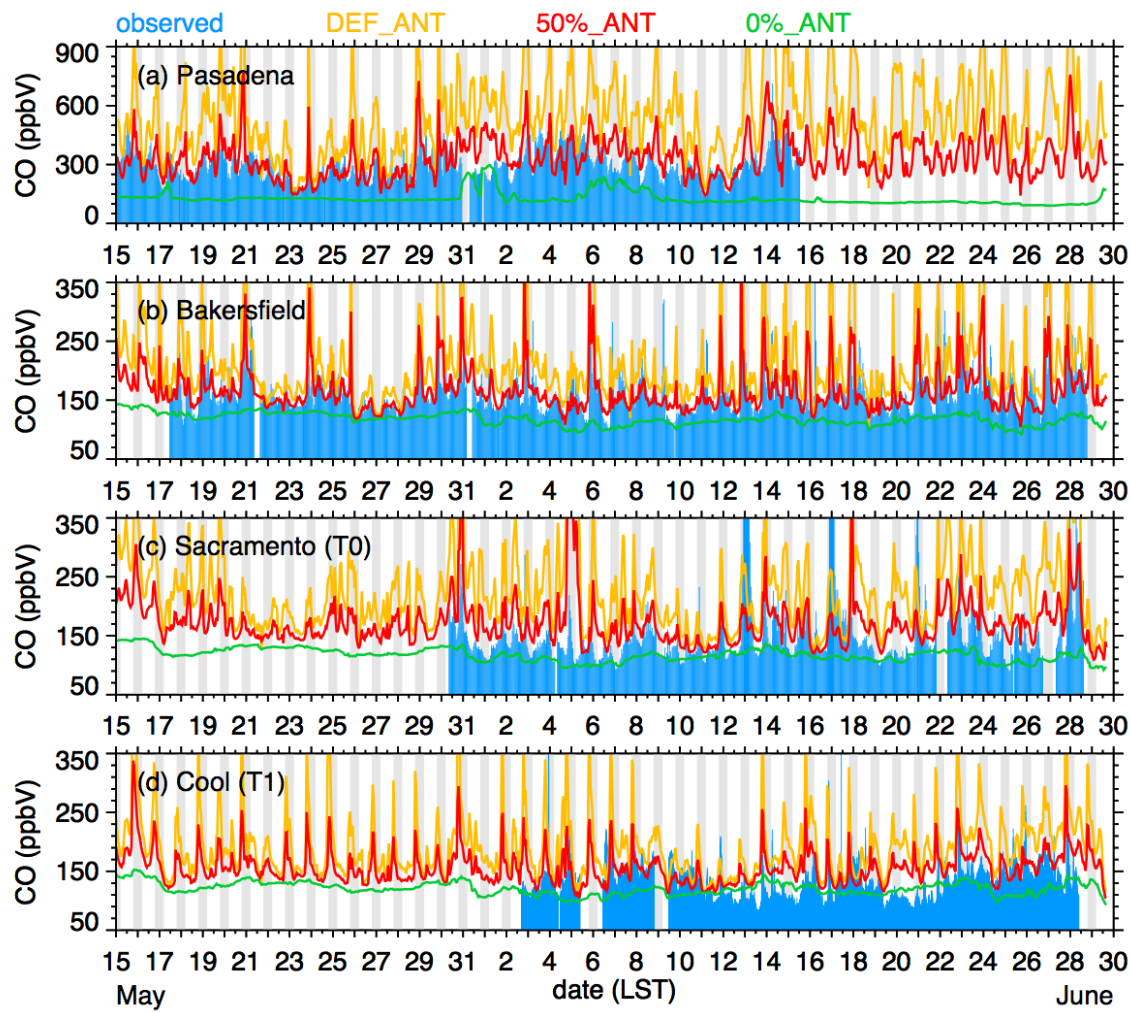


Figure S5. Observed and simulated carbon monoxide (CO) at the (a) Pasadena, (b) Bakersfield, (c) T0, and (d) T1 supersites. Gray shading denotes night.

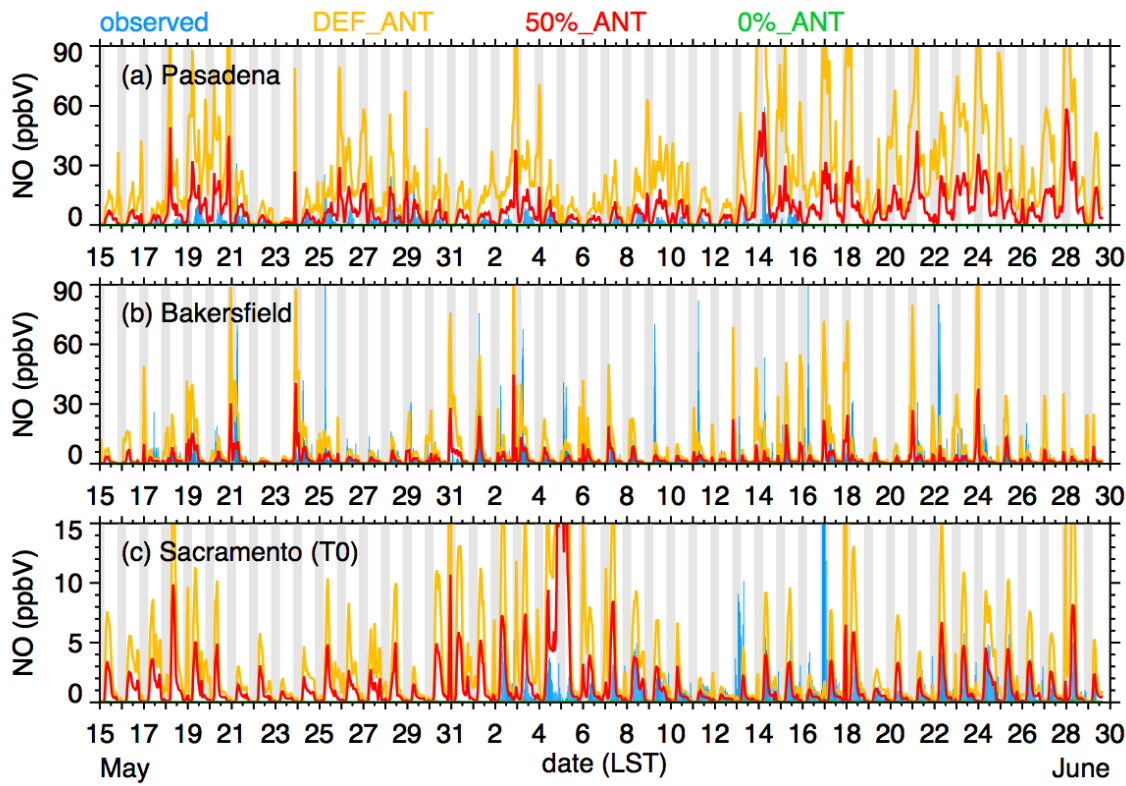


Figure S6. Observed and simulated nitrogen oxide (NO) at the (a) Pasadena, (b) Bakersfield, and (c) T0 supersites. Gray shading denotes night.

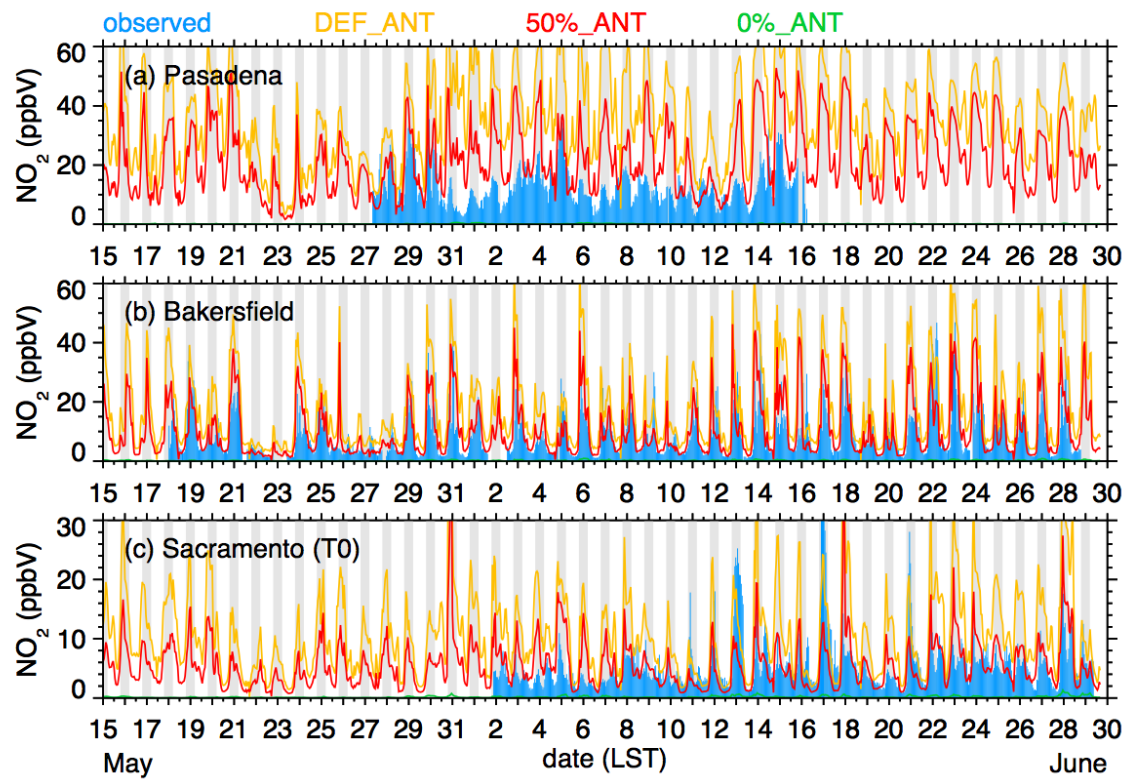


Figure S7. Observed and simulated nitrogen dioxide (NO_2) at the (a) Pasadena, (b) Bakersfield, and (c) T0 supersites. Gray shading denotes night.

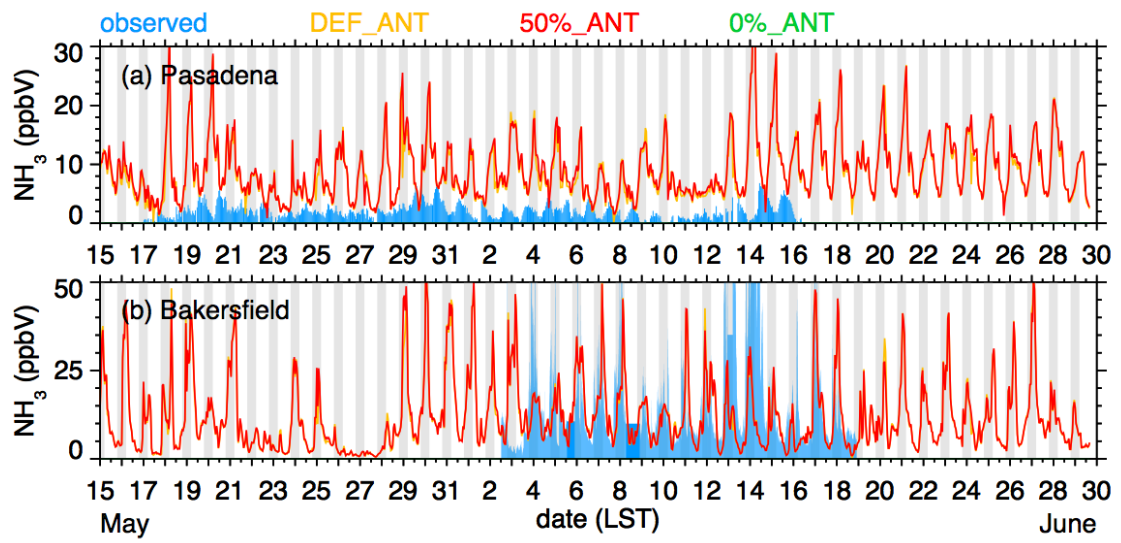


Figure S8. Observed and simulated ammonia (NH_3) at the (a) Pasadena and (b) Bakersfield supersites. Gray shading denotes night.

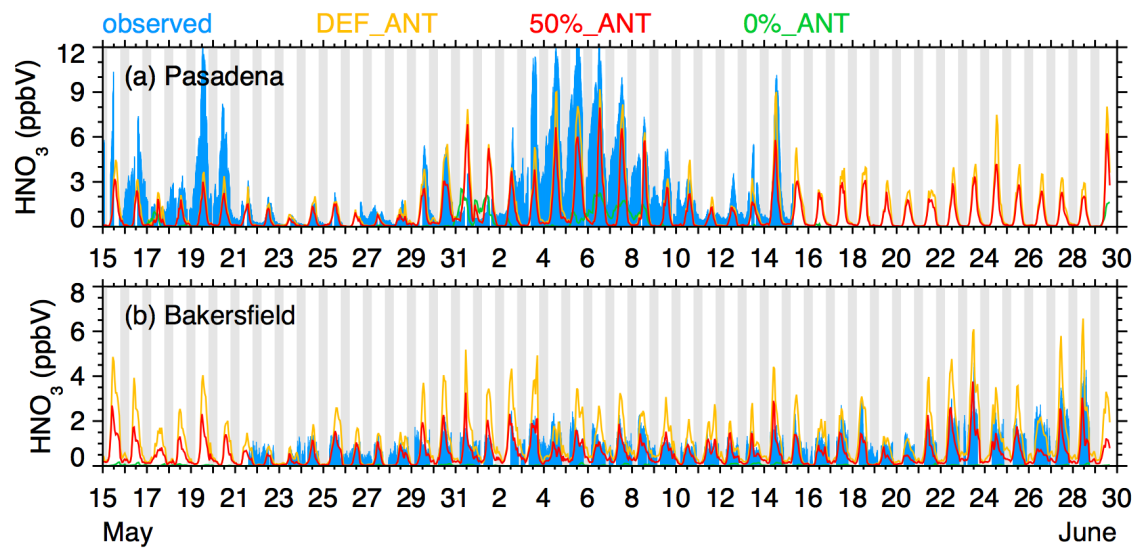


Figure S9. Observed and simulated nitric acid (HNO_3) at the (a) Pasadena and (b) Bakersfield supersites. Gray shading denotes night.

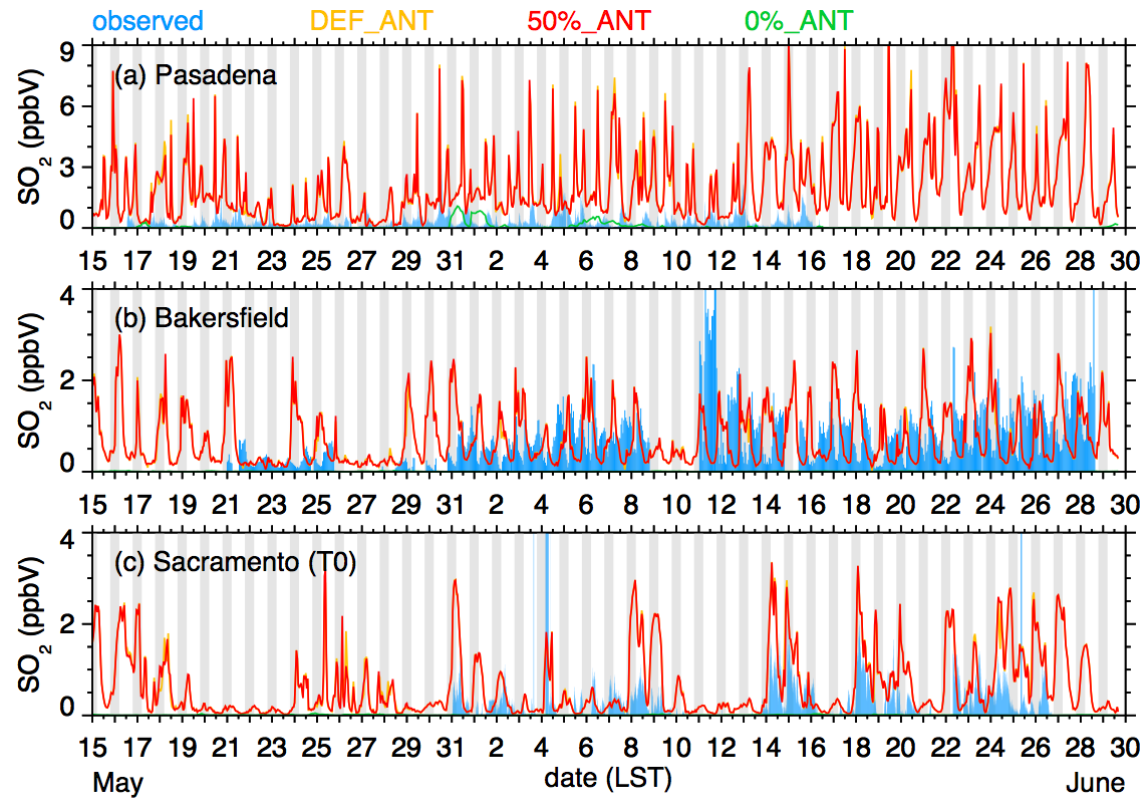


Figure S10. Observed and simulated sulfur dioxide (SO_2) at the (a) Pasadena, (b) Bakersfield, and (c) T0 supersites. Gray shading denotes night.

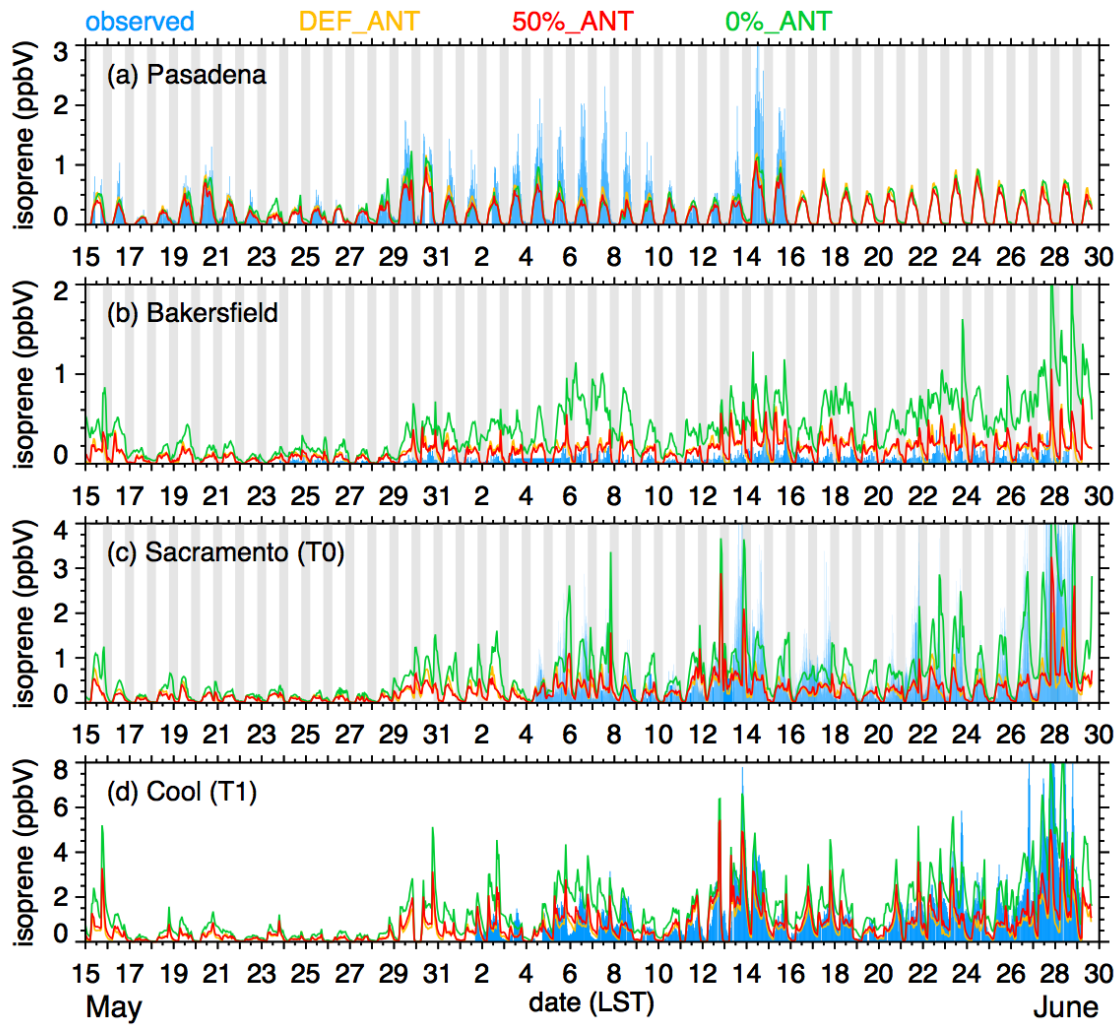


Figure S11. Observed and simulated isoprene at the (a) Pasadena, (b) Bakersfield, (c) T0, and (d) T1 supersites. Gray shading denotes night.

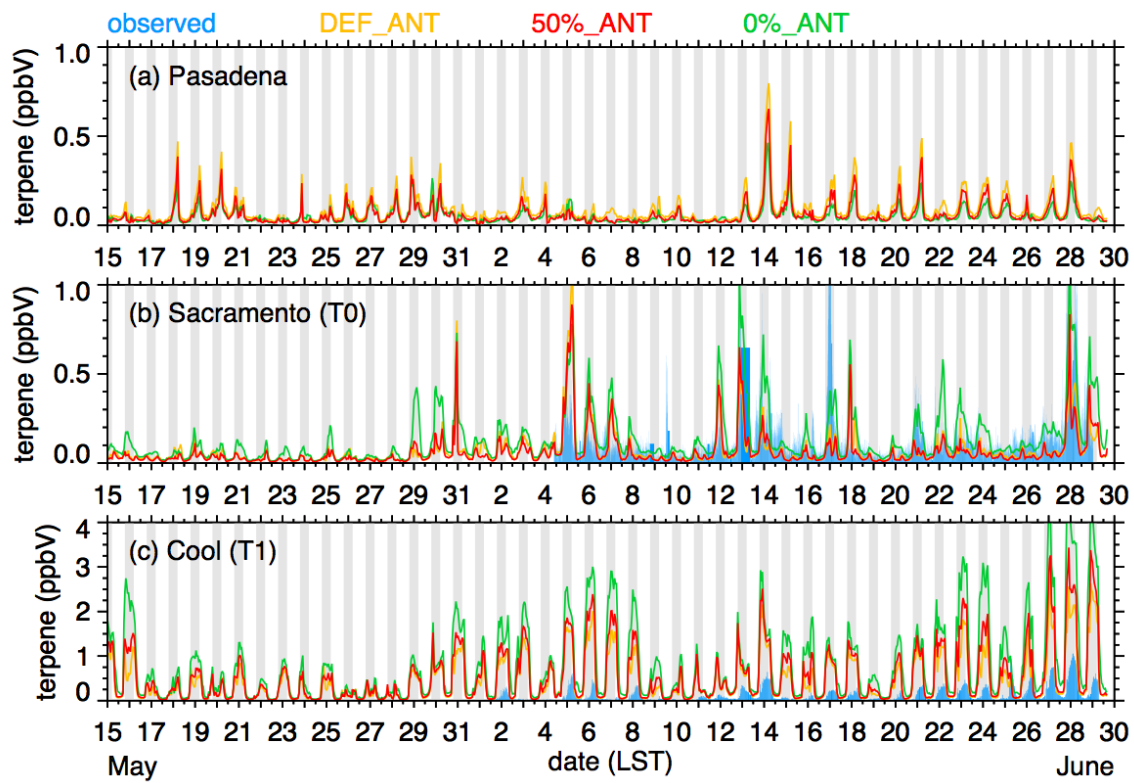


Figure S12. Observed and simulated terpene at the (a) Pasadena, (b) T0, and (c) T1 supersites. Gray shading denotes night.

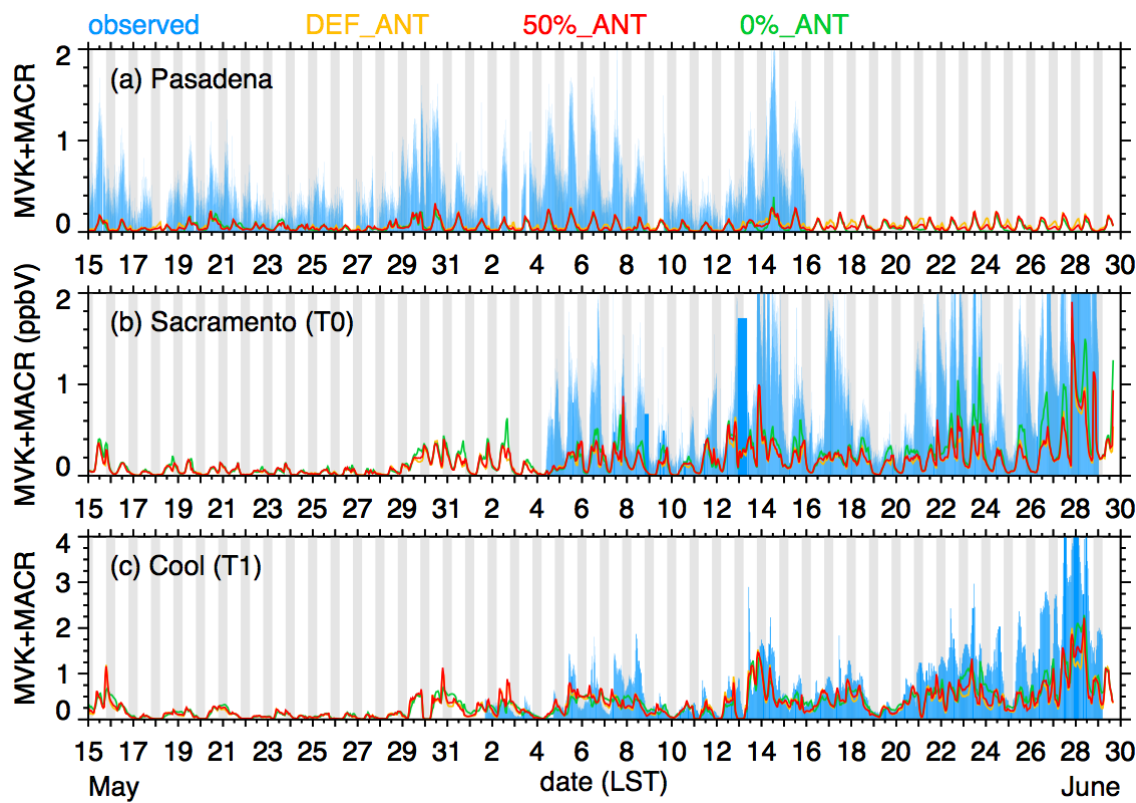


Figure S13. Observed and simulated methyl-vinyl-ketone + methacrolein (MVK+MACR) at the
(a) Pasadena, (b) T0, and (c) T1 supersites. Gray shading denotes night.

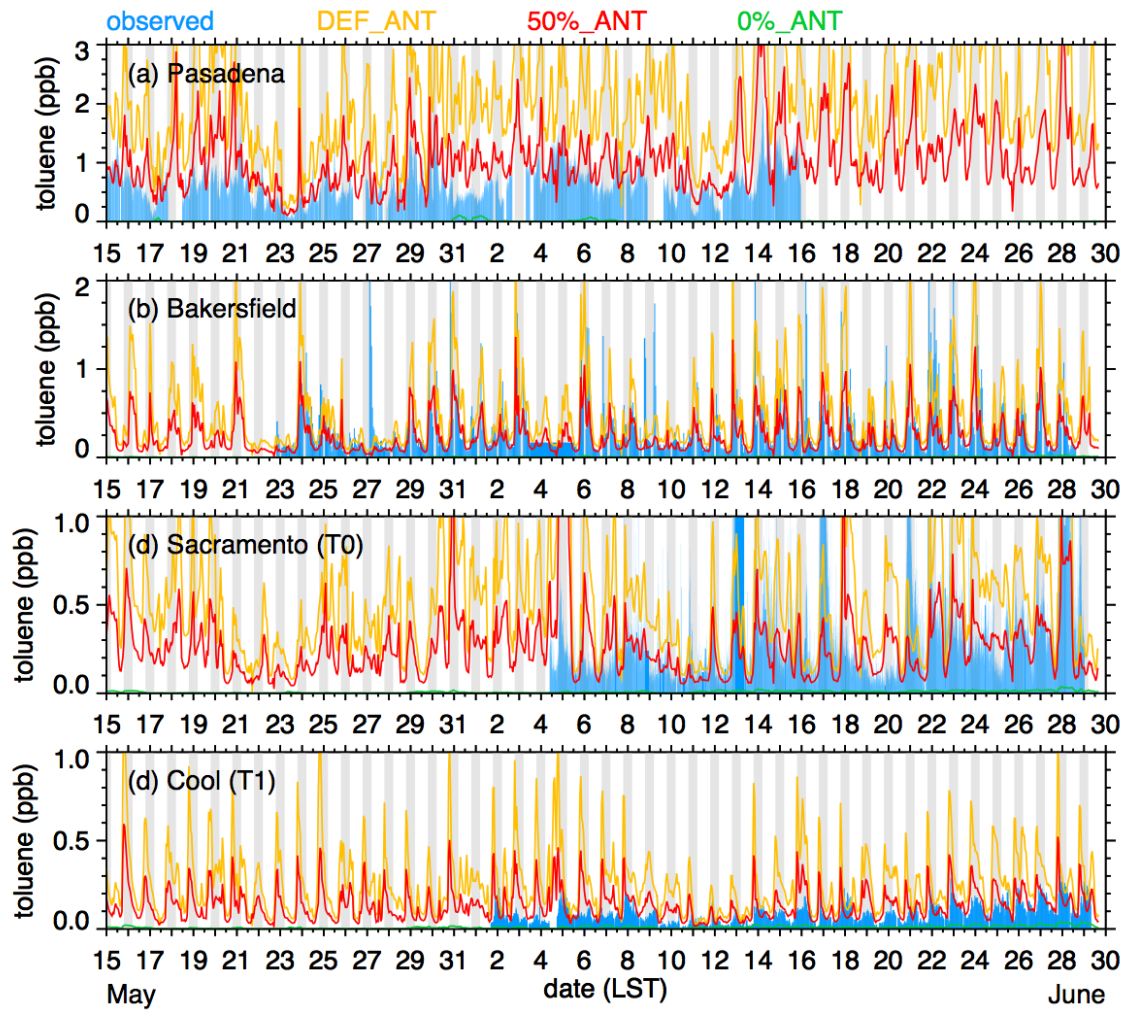


Figure S14. Observed and simulated toluene at the (a) Pasadena, (b) Bakersfield, (c) T0, and (d) T1 supersites. Gray shading denotes night.

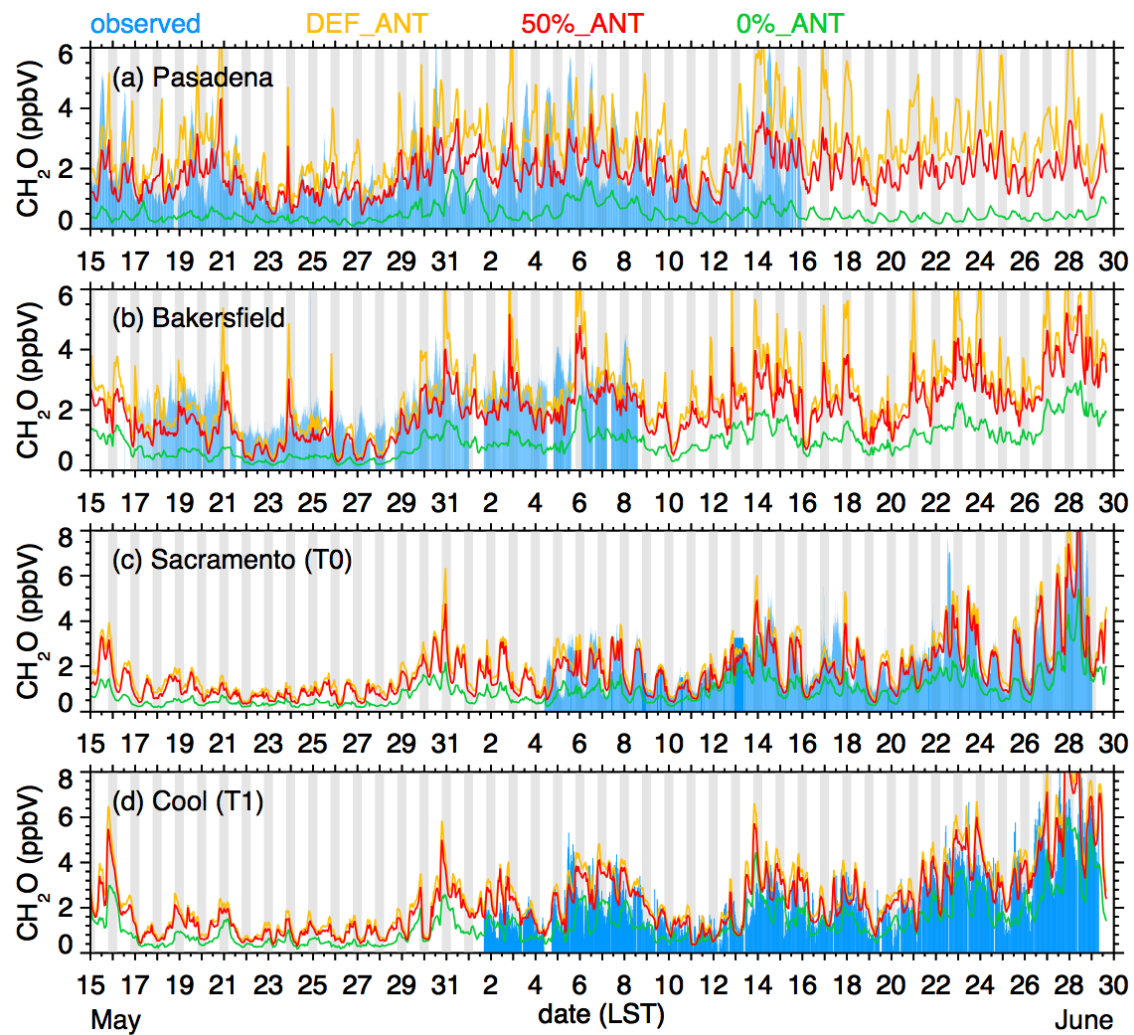


Figure S15. Observed and simulated formaldehyde (CH_2O) at the (a) Pasadena, (b) Bakersfield, (c) T0, and (d) T1 supersites. Gray shading denotes night.

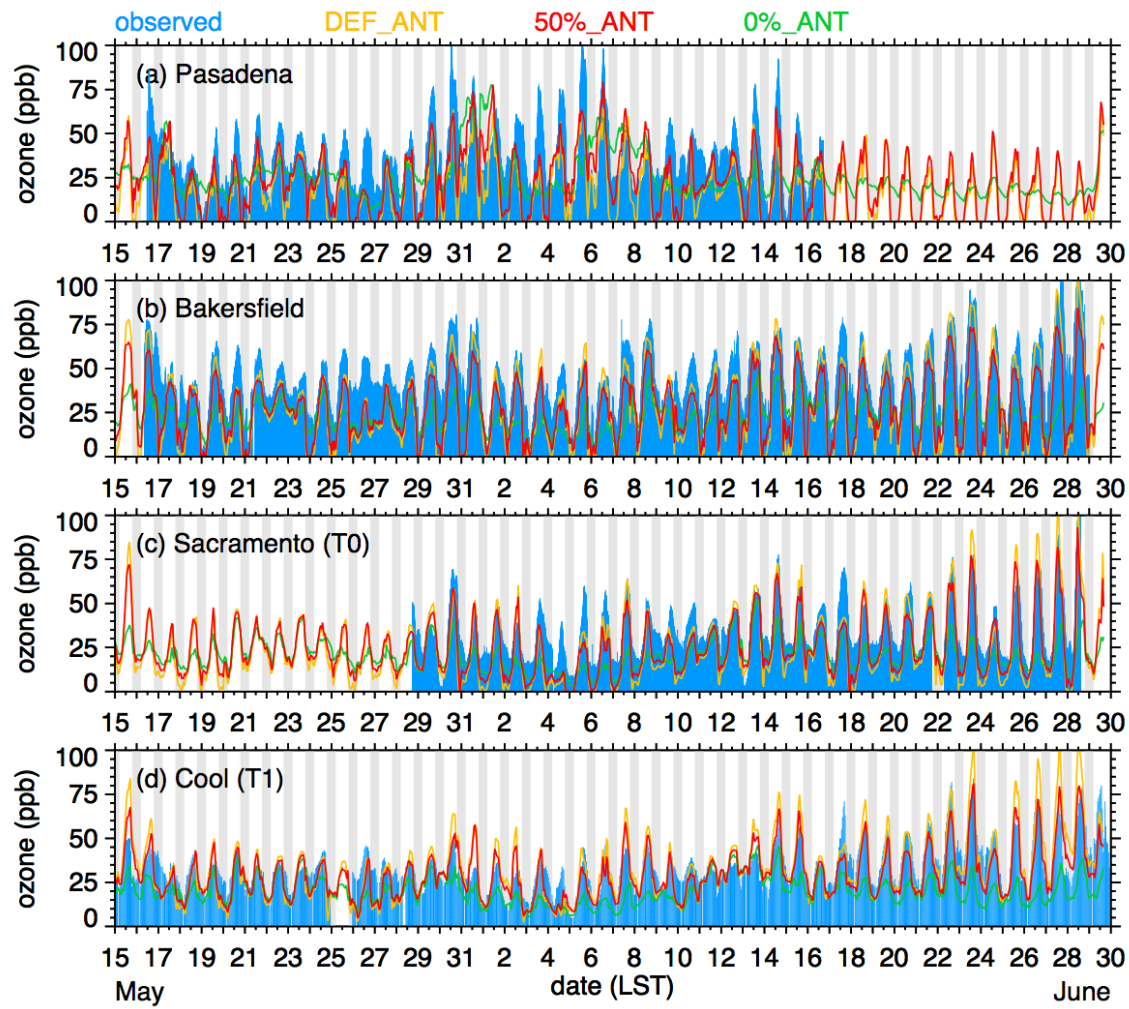


Figure S16. Observed and simulated ozone at the (a) Pasadena, (b) Bakersfield, (c) T0, and (d) T1 supersites. Gray shading denotes night.